www.nature.com/scientificreports

scientific reports

OPEN

Refined photovoltaic parameters estimation via an improved Sinh Cosh Optimizer with trigonometric operators

Ala Saleh Alluhaidan[1], Diaa Salama AbdElminaam[2]✉, Taraggy M. Ghanim[3], Sahar A. El-Rahman[4], Ibrahim Shawky Farahat[5], Arar Al Tawil[6], Yasmin Alkady[3] & Walaa H. Elashmawi[3,7]

Estimating parameters in solar cell models is crucial for simulating and designing photovoltaic systems. The single-diode, double-diode, and three-diode models represent these systems. Parameter estimation can be viewed as an optimization problem to minimize the difference between measured and estimated data. This study presents PV parameter estimation using the enhanced Sinh Cosh Optimizer (I_SCHO), incorporating trigonometric operators from the Sine Cosine Algorithm (SCA). This integration improves the algorithm's ability to navigate complex search spaces, avoid local optima, and expedite convergence. Assessment criteria include runtime, convergence behaviour, minimum RMSE, and system reliability measured by SD. Results show that I_SCHO consistently delivers superior accuracy and reliability compared to other methods. Experiments were conducted on five solar cells: RTC France, Photowatt-PWP201, Kyocera KC200GT, Ultra 85-P, and STM6-40/36 module. The study also includes a comparative analysis using state-of-the-art algorithms, demonstrating I_SCHO's efficiency through RMSE, Power Voltage (P-V) and Current Voltage (I-V) curves.

Keywords Sinh Cosh optimizer (SCHO), Trigonometric operators, Solar energy, PV parameter estimation, Single diode model, Double diode model, Three diode model

Abbreviations

PV	Photovoltaic
SCHO	Sinh Cosh Optimizer
SDM	Single diode model
DDM	Double diode model
TDM	Three diode model
TPVM	Three PV models
ALO	Ant Lion Optimizer
HGS	Hunger games search
RSO	Rat Swarm Optimizer
SOA	Seagull Optimization Algorithm
STOA	Sooty Tern Optimization Algorithm
SCA	Sine Cosine Algorithm
GWO	Grey Wolf Optimizer

[1]Departmemt of Information Systems, College of Computer and Information Science, Princess Nourah Bint Abdulrahman University, Riyadh 11671, Saudi Arabia. [2]Information Systems Department, Faculty of Computers and Artificial Intelligence, Benha University, Benha 13518, Egypt. [3]Faculty of Computer Science, Misr International University, Cairo, Egypt. [4]Computer Systems Program-Electrical Engineering Department, Faculty of Engineering-Shoubra, Benha University, Cairo 12311, Egypt. [5]Faculty of Computers and Information, Luxor University, Luxor 85951, Egypt. [6]Faculty of Information Technology, Applied Science Private University, Amman 11931, Jordan. [7]Computer Science Department, Faculty of Computers & Informatics, Suez Canal University, Ismailia 41522, Egypt. ✉email: diaa.salama@fci.bu.edu.eg

Clean energy is an indispensable component in the worldwide effort to develop sustainable and renewable energy sources. Primarily aimed at reducing environmental harm and promoting long-term sustainability, it constitutes the seventh goal within the overarching framework of renewable energy objectives. Clean energy sources include but are not limited to solar, wind, hydropower, and geothermal power. Each source significantly reduces finite fossil fuel resources and mitigates climate change. Clean energy is an indispensable component in the worldwide effort to develop sustainable and renewable energy sources. Primarily aimed at reducing environmental harm and promoting long-term sustainability, it constitutes the seventh goal within the overarching framework of renewable energy objectives. Clean energy sources include but are not limited to solar, wind, hydropower, and geothermal power. Each source contributes significantly to reducing finite fossil fuel resources and mitigating climate change[1].

Particularly for developing nations, the attainment of renewable energy represents an objective of the utmost importance. Traditional energy production methods, which frequently contribute to deforestation, greenhouse gas emissions, air and water pollution, and environmental harm, can be mitigated by adopting renewable energy sources, given the context of global energy demands. Developing countries have a distinct opportunity to bypass the environmentally detrimental phases of industrialization and promote sustainable development by embracing renewable energy technologies.

Additionally, renewable energy initiatives have the potential to bolster energy security by diversifying the energy portfolio and reducing reliance on volatile fossil fuel markets. Subsequently, this assists nations that may encounter difficulties stemming from volatile energy prices in bolstering their economic stability and resilience.

Advancing sustainable energy is consistent with worldwide initiatives to fulfill the Sustainable Development Goals (SDGs) established by the United Nations and its environmental and economic advantages. Access to affordable, pure energy is vital to combat poverty, improve health, and advance education in developing countries. Nations can foster economic expansion, furnish their populace with dependable and environmentally sustainable energy, and generate employment prospects through investments in renewable energy infrastructure.

Acquiring sustainable energy is an all-encompassing strategy that profoundly impacts worldwide progress rather than solely an environmental objective. Particularly significant for the socioeconomic advancement of developing countries, it signifies a dedication to a more resilient, sustainable, and equitable future. The global transformative influence of renewable energy becomes progressively apparent as the international community collaborates to achieve these goals.

Ongoing increases in electricity consumption have resulted from the tremendous growth of the global economy. The substantial consumption of coal and oil has resulted in immediate blackouts of electricity and increased atmospheric emissions. The electricity problem coincides with the nation's economy's most challenging development phase. Solar photovoltaic (PV) systems have recently garnered considerable interest as a solution to these crises. The process by which photovoltaic cells transform solar energy into electrical energy is currently undergoing significant advancements[2–4]. An equivalent circuit of these PV cells is required to evaluate the properties of the cells under different operating conditions. For parameter estimation problems, the single-diode model (SDM) and the double-diode model (DDM) have been extensively documented and proposed in the literature. These models are widely used and preferred[5,6]. Solar PV cells being exposed to the external environment diminishes the cells' and the system's overall efficacy. As the overall performance of the PV system is highly dependent on uncertain parameters, it is crucial to estimate the ideality factor (a), series resistance (Rse), photocurrent (Ip), reverse saturation current of the diode (Isd), and shunt resistance (Rsh) for SDM; and photocurrent (Ip), reverse saturation current of the two diodes (Isd1 and Isd2), shunt resistance (Rsh), and series resistance (Rse) for DDM. However, the existing equations utilized in both SDM and DDM photovoltaic models are transcendental, which presents challenges in estimating cell variables and analyzing the performance of the cell or module, as previously stated. Therefore, it is imperative to develop a methodology that can efficiently and effectively calculate the cell/module parameters[7,8] Conversely, estimation of their unknown parameters utilizing I-V measured data is required when employing SD and DD models. The configurations of these parameters directly impact the efficiency of solar PV cells[9]. The utilization of optimization techniques to ascertain the unknown parameters of PV models has been demonstrated to be both practical and efficient[10,11]. Developing an appropriate fitness evaluation function can conceptualize the estimation of PV model parameters as an optimization problem involving multidimensional functions[12]. Nevertheless, the I-V characteristics of PV models determine the fitness function.

I-V data does contain some degree of noise interference because it is acquired through measurement. Therefore, the optimization problem's search space is exceedingly complex, multimodal, multivariable, and nonlinear[13]. Two optimization techniques are utilized in estimating parameters for photovoltaic (PV) systems: conventional optimization approaches and contemporary metaheuristic algorithms. Lambert W-function approaches[14–18] ,Newton methods[19,20], the tabular method[21], the iterative curve fitting method[22], and so forth are examples of conventional optimization techniques. Nevertheless, traditional optimization methods frequently possess certain constraints. For instance, the performance of the problem is contingent upon its initial values, the fitness function must be convex, continuous, and derivable, and it is simple to enter a local optimum. Modern meta-heuristic approaches are optimization techniques based on population iteration. These methods can efficiently resolve complex optimization problems because of their straightforward implementation and underlying principle. In recent decades, researchers have devised numerous enhanced iterations of meta-heuristic algorithms to estimate the unknown parameters of PV models accurately. For example, back-tracking search algorithm (BSA)[12,23], butterfly optimization algorithm (BOA) [10], slime mold optimizer (SMO)[15,24], marine predators algorithm (MPA)[15,25,26], JAYA algorithm[27–29], Jellyfish search optimizer (JSO)[30], differential evolution (DE)[31,32], coyote optimization algorithm (COA)[33], wind-driven optimization (WDO)[34], radial movement optimization (RMO)[35], teaching-learning-based optimization (TLBO)[36], grasshopper optimization algorithm (GOA)[37], Harris hawks optimizer (HHO)[38,39], equilibrium optimizer (EO)[40], bat algorithm (BA)[41], cuckoo search optimization (CSO)[42], transient search optimization (TSO)[43], moth flame optimization (MFO)[44], particle swarm optimizer (PSO)[45,46], electromagnetic-like algorithm (ELA)[47], tree growth algorithm (TGA)[48], sunflower optimization (SFO)[49], whale optimization algorithm (WOA)[50–52], bacterial foraging optimization (BFO)[53], ant lion optimizer (ALO)[54], simplified swarm optimization (SSO)[55], artificial bee colony (ABC)[56], genetic algorithm (GA)[57], biogeography-based optimization (BBO)[58], sine cosine algorithm (SCA)[59], salp swarm algorithm (SSA)[60], water cycle algorithm (WCA)[61], bird mating optimizer (BMO)[62], imperialist competitive algorithm (ICA)[63], multi-verse optimizer (MVO)[64], and so on. These enhanced meta-heuristic algorithms yield satisfactory outcomes when estimating parameters for PV models. Nevertheless, an algorithm can never be flawless. Consequently, it is imperative to devise an enhanced meta-heuristic optimization methodology to approximate the unidentified parameters of solar PV models.

Most researchers have been engaged in estimating the parameters of three PV models (single diode, double diode, and three diode models) utilizing optimization algorithms. Ongoing development efforts are devoted to optimizing algorithms to attain optimal accuracy for the objective function. Prior research has endeavored to develop a PV model capable of producing current data comparable to experimental data.

The following items summarized the contributions of this paper:

- Introducing the Sinh Cosh optimizer (SCHO) designed to identify unspecified DDM, TDM, and SDM parameters.
- Enhancing the SCHO algorithm by integrating trigonometric op-operators inspired by the Sine Cosine Algorithm (SCA) into the exploitation phase to improve convergence speed and avoid local optima, resulting in a more precise estimation of unknown parameters.
- Conducting a comparative analysis of I_SCHO against various competitors to gauge its effectiveness.
- Experimental results indicate that I_SCHO surpasses all compared techniques, producing significantly different and superior outcomes.The rest of the sections are organized as follows: "Problem formulation" section discusses the modeling of PV models. "A Sinh Cosh optimizer" section explains the problem formulation. "Enhanced Sinh Cosh optimizer with trigonometricoperators (I_ SCHO)" section analyses the Sinh Cosh optimizer (SCHO) algorithm. In "Results and simulation" section, the simulation and results are discussed. The conclusions of this paper are presented in "Conclusion" section.

Definition of PV models

This section discusses the mathematical analysis of the three PV models (TPVM) and the modified three (MTPVM) models. The TPVM includes a single diode model (SDM), a double diode model (DDM), and a three diode model (TDM). Meanwhile, the MTPVM contains a modified single-diode model (MSDM), a modified double-diode model (MDDM), and a modified three-diode model (MTDM).

Single diode model

Figure 1 illustrates the equivalent circuit of SDM. The current output in this model is determined through the application of the subsequent equation:

$$I = I_{pv} - I_{D1} - I_{sh} \tag{1}$$

$$I = I_{pv} - I_{o1}\left[e^{\frac{q(V+IR_s)}{n_1 KT_c}} - 1\right] - \frac{V + IR_s}{R_p} \tag{2}$$

The SDM produces a current denoted as *I*, where *Ipv* represents the generated light current, *Ish* signifies the leakage current, and *ID*1 stands for the dark saturation current. *Rp* and *Rs* represent the shunt and series resistances, respectively. Additionally, *n*1 is the diode ideality factor, *K* is Boltzmann's constant, *q* represents the charge of an electron, and *Tc* denotes the cell temperature. According to the provided mathematical formula, the parameters to be estimated in SDM include *Ipv*, *Io*1, *n*1, *Rs*, and *Rp*.

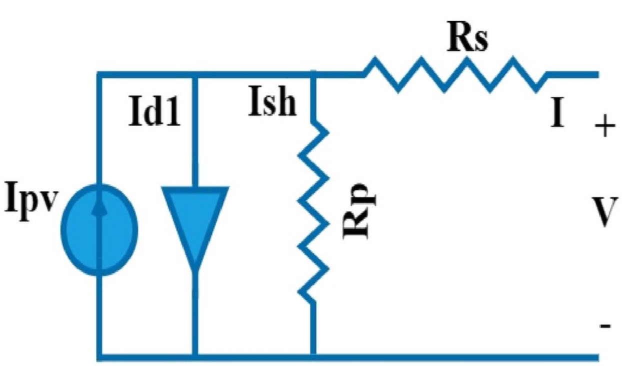

Fig. 1. Equivalent circuit for single diode model.

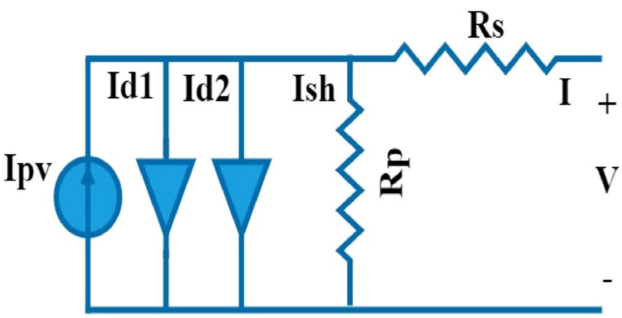

Fig. 2. Equivalent circuit for double diode model.

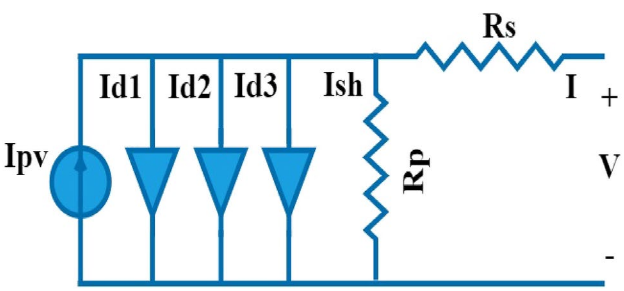

Fig. 3. Equivalent circuit for three diode model.

Double diode model
Figure 2 depicts the electrical diagram for the DDM, employing two diodes to enhance output quality. The following equations determine the current output in this model:

$$I = I_{pv} - I_{D1} - I_{D2} - I_{sh} \tag{3}$$

$$I = I_{pv} - I_{o1}\left[e^{\frac{q(V+IR_s)}{n_1 KT_c}} - 1\right] - I_{o2}\left[e^{\frac{q(V+IR_s)}{n_2 KT_c}} - 1\right] - \frac{V+IR_s}{R_p} \tag{4}$$

where *ID*2 denotes the dark saturation current of the second diode, and *n*2 represents the ideality factor of the second diode. The model involves seven parameters to be estimated: *Ipv*, *Io*1, *n*1, *Rs*, *Rp*, *Io*2, and *n*2.

Three diode model
The three-diode model (TDM) illustrated in Fig.3 offers an alternative approach for designing PV modules, incorporating three diodes. The computation of the current output in this model is carried out through Eq. (5):

$$I = I_{pv} - I_{D1} - I_{D2} - I_{D3} - I_{sh} \tag{5}$$

$$I = I_{pv} - I_{o1}\left[e^{\frac{q(V+IR_s)}{n_1 KT_c}} - 1\right] - I_{o2}\left[e^{\frac{q(V+IR_s)}{n_2 KT_c}} - 1\right] - I_{o3}\left[e^{\frac{q(V+IR_s)}{n_3 KT_c}} - 1\right] - \frac{V+IR_s}{R_p} \tag{6}$$

Where *ID*3 denotes the dark saturation current of the third diode, and *n*3 represents the ideality factor of the third diode. The TDM involves estimating nine parameters: *Ipv*, *Io*1, *n*1, *Rs*, *Rp*, *Io*2, *n*2, *Io*3, and *n*3.

Problem formulation
The TPVM's performance is evaluated based on objective functions, specifically the root mean square error (RMSE) objective functions, which quantify the disparity between the current computed using estimated parameters and the current from the dataset. Equations 7 and 8 articulate the definition of RMSE:

$$J\left(V,\ I,\ X\right) = I - I_{exp} \tag{7}$$

$$RMSE = \sqrt{\frac{1}{N}\sum_{i=1}^{N}\left(J\left(V,\ I,\ X\right)\right)^2} \tag{8}$$

Here, I_{exp} represents the experimental current, N denotes the number of data readings, and X encompasses the decision variables.

The vector of decision variable for SDM is $X = \{(I_{pv},\ I_{o1},\ n_1,\ R_s\ and\ R_p\ )\}$.
The vector of decision variable for DDM is $X = \{(I_{pv},\ I_{o1},\ n_1,\ R_s,\ R_p,\ I_{o2}\ and\ n_2\ )\}$.
The vector of decision variable for TDM is $X = \{(I_{pv},\ I_{o1},\ n_1,\ R_s,\ R_p,\ I_{o2},\ n_2,\ I_{o3}\ and\ n_3)\}$.

The TPVM parameters can be estimated through optimization algorithms. This study utilizes data from the R.T.C France solar cell for TPVM information. The Enhanced Sinh Cosh Optimizer (I_SCHO) algorithm, recently introduced, is employed. The outcomes are compared with various algorithms, including the Grey Wolf Optimizer (GWO)[65], Ant Lion Optimizer (ALO)[54], Sine Cosine Algorithm (SCA)[66], Sooty Tern Optimization Algorithm (STOA)[67], Tunicate Swarm Algorithm (TSA)[68], Hunger Games Search (HGS)[69], Rat Swarm Optimizer (RSO)[70], and Sinh Cosh Optimizer (SCHO)[71]. The search space boundaries for parameter estimation using the R.T.C France solar cell are detailed in Table 1[12].

A Sinh Cosh Optimizer

The Sinh Cosh Optimizer (SCHO) is a novel meta-heuristic optimization algorithm inspired by the characteristics of the hyperbolic functions Sinh and Cosh[72]. It is designed to balance exploration and exploitation in optimization problems by utilizing a mathematical model with phases of exploration and exploitation, a bounded search strategy, and a switching mechanism. SCHO has shown strong performance in solving benchmark functions and engineering design problems compared to other well-known meta-heuristic algorithms. The following subsection illustrates the basic steps of the SCHO.

Phase of initialization

Random initialization To commence, the algorithm initializes a set of candidate solutions randomly according to Eq. (9).

$$X = \mathrm{rand}(N, \mathrm{dim}) \times (ub - lb) + lb \tag{9}$$

where *dim* denotes the dimension of problem variables, *N* is the number of solutions, *ul*, and *lb* are the upper and lower bounds of variables, respectively, and *rand* is a generated random number in the range 0 and 1.

The aforementioned preliminary solutions function as the foundation for the process of optimization. Candidate solutions are pivotal in instigating the exploration and exploitation phases as they symbolize prospective resolutions to the optimization problem.

Exploration stage

Extensive search In the exploration phase, the algorithm searches the solution space to identify novel regions that might harbor optimal solutions. This process involves two subphases, and switching between them is given by Eq. (10).

$$T = floor\left(\frac{Max\_iteration}{ct}\right) \tag{10}$$

where *ct* is a coefficient for establishing the switching point in two phases, fixed at 3.6. $Max\_iteration$ is the maximum iteration rounds. *floor* denotes a function used for rounding down.

- Exploration (phase 1): Early iterations will focus on exploring the outside edges of the search space close to the search agents' positions, while later iterations will bring the agents closer to the optimal answer. The updated position at this stage is done according to Eq. (11)

$$X_{(i,j)}^{t+1} = \begin{cases} X_{best}^{(j)} + r_1 \times W_1 \times X_{(i,j)}^{t} & \text{if } r_2 > 0.5 \\ X_{best}^{(j)} - r_1 \times W_1 \times X_{(i,j)}^{t} & \text{if } r_2 < 0.5 \end{cases} \tag{11}$$

Where:

Parameters	Lower bound	Upper bound
I_{pv}	0	1
$I_{o1},\ I_{o2}\ and\ I_{o3}\ \ (\mu A)$	0	1
$R_s,\ R_{s1}$	0	0.5
R_p	0	100
$n_1,\ n_2\ and\ n_3$	1	2

Table 1. The limits of estimated parameters[12].

- $X_{(i,j)}^{t}$ and $X_{(i,j)}^{t+1}$ represent the current and updated position of the *j*th dimension of the *i*th solution.
- $X_{best}^{(j)}$ denotes the best position achieved so far in the optimization process in the *j*th dimension.
- r_1 and r_2 are random numbers in the interval [0, 1]. These random values introduce stochasticity into the position update process.
- W_1 is the weight coefficient for controlling candidate solutions' search space exploration. It can be calculated based on Eqs. (12) and (13) where a_1 is a monotonically decreasing function and r_3 and $r_4 \in [0, 1]$. *u* and *m* are sensitive coefficients that regulate the accuracy of the exploration process.

$$W_1 = r_3 \times a_1 \times (\cosh r_4 + u \times \sinh r_4 - 1) \tag{12}$$

$$a_1 = 3 \times \left(-1.3 \times \frac{t}{Max\_iteration} + m\right) \tag{13}$$

- Exploration (phase 2): Search agents exhibit minimal sensitivity to the optimal solution and, as a result, navigate in a non-directional manner toward the subsequent position using their current location as a guide. This can be done through Eq. (14)

$$X_{(i,j)}^{t+1} = \begin{cases} X_{(i,j)}^{t} + \left| \varepsilon \times W_2 \times X_{best}^{(j)} - X_{(i,j)}^{t} \right| & \text{if } r_5 > 0.5 \\ X_{(i,j)}^{t} - \left| \varepsilon \times W_2 \times X_{best}^{(j)} - X_{(i,j)}^{t} \right| & \text{if } r_5 < 0.5 \end{cases} \tag{14}$$

Where:

- $X_{(i,j)}^{t+1}$ and $X_{(i,j)}^{t}$ represent the updated and current position of the *j*th dimension of the *i*th solution.
- $X_{best}^{(j)}$ denotes the best position achieved.
- ε is a tiny positive number set to 0.003 based on the experiments.
- W_2 is the weight coefficient calculated using Eqs. (15) and (16) where a_2 is a monotonically decreasing function and r_5 and $r_6 \in [0, 1]$. *n* is a sensitive coefficient that regulates the accuracy of the exploration process.

$$W_2 = r_6 \times a_2 \tag{15}$$

$$a_2 = 2 \times \left(-\frac{t}{Max\_iteration} + n\right) \tag{16}$$

The exploitation stage

Enhanced search To improve solution quality, candidate solutions are modified to take advantage of identified regions and refine the search for the optimal solution. This process includes two phases, as described below.

- Exploitation (phase one): X's closest neighbor is targeted in the initial exploitation stage. Therefore, update the position according to Eq. (17).

$$X_{(i,j)}^{t+1} = \begin{cases} X_{best}^{(j)} + r_7 \times W_3 \times X_{(i,j)}^{t} & \text{if } r_8 > 0.5 \\ X_{best}^{(j)} - r_7 \times W_3 \times X_{(i,j)}^{t} & \text{if } r_8 < 0.5 \end{cases} \tag{17}$$

Where:

- $X_{(i,j)}^{t}$, $X_{(i,j)}^{t+1}$, and $X_{best}^{(j)}$ represent the current and updated position and the best solution, respectively, which are defined before.
- r_7 and r_8 are two random numbers generated in the interval [0, 1].
- W_3 is the weight coefficient that controls the search space around the potential solutions, ranging from close to far. It can be calculated based on Eq. (18). a_1 computed according to Eq. (13) and r_9 and r_{10} $\in [0, 1]$. *u* as defined before in the exploration phase.

$$W_3 = r_9 \times a_1 \times (\cosh r_{10} + u \times \sinh r_{10}) \tag{18}$$

- Exploitation (phase two): candidate solutions will deeply exploit the best solution produced so far, intensifying exploitation as iterations increase. As a result, the update position is done according to Eq. (19)

$$X_{(i,j)}^{t+1} = X_{(i,j)}^{t} + r_{11} \times \frac{\sinh r_{12}}{\cosh r_{12}} \left| W_2 \times X_{best}^{(j)} - X_{(i,j)}^{t} \right| \tag{19}$$

where r_{11} and $r_{12} \in [0,1]$, W_2 computed before according to Eq. (15) while $\frac{\sinh r_{12}}{\cosh r_{12}}$ is employed to retain potential solutions' diversity.

The bounded search strategy

To fully use the possible search space, an approach similar to animal hunting in the latter stage is applied in SCHO, known as the bounded search strategy. To thoroughly explore and utilize the potential space, all candidate solutions are randomly started in this potential space by utilizing Eq. (9). Then, the space will be extensively investigated and utilized. Further, the initialization of the bounded search strategy can be computed by applying Eq. (20) where the value of BS_k is computed according to Eq. (21) starting at $k = 1$.

$$BS_{k+1} = BS_k + floor\left(\frac{Max\_iteration - BS_k}{\alpha}\right) \tag{20}$$

$$BS_1 = floor\left(\frac{Max\_iteration}{\beta}\right) \tag{21}$$

The value of α, set to 4.6, indicates a sensitive coefficient that governs the accuracy of thorough exploration and exploitation in the potential space. While the value that initiates the bounded search strategy is controlled by β and is set to 1.55. When SCHO employs the bounded search technique every time, the upper *ub* and lower bounds *lb* of decision variables will be determined using Eqs. (22) and (23) based on the *j*th best and suboptimal solutions.

$$lb_k = X_{best}^{(j)} - \left(1 - \frac{t}{Max_i teration}\right) \times \left| X_{best}^{(j)} - X_{\text{second}}^{(j)} \right| \tag{22}$$

$$ub_k = X_{best}^{(j)} + \left(1 - \frac{t}{Max_i teration}\right) \times \left| X_{best}^{(j)} - X_{second}^{(j)} \right| \tag{23}$$

Switching among exploration and exploitation

To achieve exploration and exploitation of the whole search space and escape from the local optimum in the later iteration, the switching mechanism should largely focus on exploration but conduct a modest amount of exploitation in the early iterations. In contrast, in the latter iterations, the switching mechanism should mostly focus on the exploitation but do a minor exploration. This can be achieved by using Eqs. (24) and (25)

$$A = \left(p - q \times \left(\frac{t}{Max\_iteration}\right)^{SC}\right) \times r_{13}. \tag{24}$$

$$SC = \frac{cosh\left(\frac{t}{Max\_iteration}\right)}{sinh\left(\frac{t}{Max\_iteration}\right)} \tag{25}$$

where *p* and *q* are the balancing coefficients for managing the exploration and exploitation throughout iterations, and r_{13} is a random value in the interval zero and one.

The overall steps of the SCHO are illustrated in algorithm 1

Data: Control parameters CP, population size N, dimension of problem variable dim, boundary search value BS_1, and maximum number of iterations $Max\_iteration$

Result: The fittest solution so far X_{best}

Procedure SCHO (CP,N,dim,BS_1,$Max\_iteration$)

Set the iteration number $t = 1$ and $k = 1$ Generate random initial population Evaluate each candidate solution X and assign the fittest one to X_{best}

while $t <= t_{max}$ **do**

  for $i = 1 : N$ **do**

    for $j = 1 : dim$ **do**

      Update the switching parameter A using Eq. 24 **if** $(t = BS_k)$ **then**

        Obtain the position of second candidate solution Update the value of BS_k according to Eq. 20 Update the entire search space with Eqs. 22 and 23 Distribute the solution space according to Eq. 9

      if $(A > 1)$ **then**

        Update the value of W_1 using Eq. 12 Update the value of W_2 using Eq. 15 **if** $(t <= T)$ **then**

          Exploration (phase one): Update the position of the candidate solution using Eq. 11

        else

          Exploration (phase two): Update the position of the candidate solution using Eq. 14

        end

      else

        Update W_3 according to Eq. 18 **if** $(t <= T)$ **then**

          Exploitation (phase one): Update the position of the candidate solution using Eq. 17

        else

          Exploitation (phase two): Update the position of the candidate solution using Eq. 19

        end

      end

    end

  end

  Compute the fitness value of each solution Update the best solution Set $t = t+1$

end

return *The fittest solution so far* X_{best}

Algorithm 1. The algorithmic steps of SCHO algorithm.

Enhanced Sinh Cosh Optimizer with trigonometric pperators (I_ SCHO)

This section outlines the methodology for enhancing the exploitation stage of the SCHO using trigonometric operators inspired by the Sine Cosine Algorithm (SCA).

- *Trigonometric operators:* The addition of sin and cos functions to dynamically update agent positions near the current best solution, enhancing local search capabilities and aiding in avoiding local optima.
- *Adaptive coefficients:* $\alpha(iter)$ and $\gamma(iter)$ are designed to adjust the influence of trigonometric updates over iterations, promoting a balance between exploration and exploitation phases.

Step 1: Initialization

Initialize a population of solutions X_i, for $i = 1, 2, \ldots, N$, within the search space. Randomly assign values to the parameters of the triple-diode photovoltaic model within the permissible bounds.

Step 2: Evaluation

Evaluate the fitness of each solution using an objective function, typically the root mean square error (RMSE) between the model output and actual data.

Step 3: Enhanced Exploitation Using Trigonometric Operators
For each solution in the population, calculate new positions using trigonometric updates:

$$X_{i,new} = X_{best} + \alpha(iter) \cdot \sin(\theta) \cdot |\beta \cdot X_{best} - X_i| + \gamma(iter) \cdot \cos(\phi) \cdot |\delta \cdot X_{best} - X_i|$$

Step 4: Update and Selection
Update the position of each solution in the population to its new position if the new position has a better fitness value than the current one. Update the best solution X_{best} if any new solution has a better fitness value.

Step 5: Adaptive adjustments
Adaptively adjust $\alpha(iter)$ and $\gamma(iter)$ based on the optimization progress to smoothly transition from exploration to exploitation.

Step 6: Termination
Repeat steps 3 to 5 until a termination criterion is met, such as reaching a maximum number of iterations or achieving a predefined level of accuracy.

Input: N: Number of agents, D: Problem dimension, $MaxIter$: Maximum iterations, $X_{\min}$, $X_{\max}$: Bounds, $ObjFunc$: Objective function
Output: X_{best}: Best solution
Initialize agents X_i randomly within $[X_{\min}, X_{\max}]$ Evaluate $ObjFunc$ for all agents to determine X_{best}
for $t = 1$ **to** $MaxIter$ **do**
  foreach *agent* X_i **do**
    Generate random angles $\theta, \phi \in [0, 2\pi]$ Calculate adaptive coefficients $\alpha(t)$ and $\gamma(t)$ $X_{i,new} = X_{best} + \alpha(t) \cdot \sin(\theta) \cdot |\beta \cdot X_{best} - X_i| + \gamma(t) \cdot \cos(\phi) \cdot |\delta \cdot X_{best} - X_i|$
    if $ObjFunc(X_{i,new}) < ObjFunc(X_i)$ **then**
      $X_i = X_{i,new}$ **if** $ObjFunc(X_i) < ObjFunc(X_{best})$ **then**
        $X_{best} = X_i$
      end
    end
  end
  Adaptively adjust $\alpha(t)$ and $\gamma(t)$ for exploitation focus
end
return X_{best}

Algorithm 2. Enhanced Exploitation Stage of SCHO with Trigonometric Operators (I_SCHO)

Input: N: Number of agents, D: Problem dimension, $MaxIter$: Maximum number of iterations, $X_{\min}$, $X_{\max}$: Search space bounds
Output: X_{best}: Best solution found
Initialize N agents X_i randomly within $[X_{\min}, X_{\max}]$ Evaluate $ObjFunc$ for all agents and determine X_{best}
for $t = 1$ **to** $MaxIter$ **do**
  for $i = 1$ **to** N **do**
    Generate random angles θ and ϕ in $[0, 2\pi]$ Calculate adaptive coefficients $\alpha(t)$ and $\gamma(t)$ $X_{new} = X_{best} + \alpha(t) \cdot \sin(\theta) \cdot |\beta \cdot X_{best} - X_i| + \gamma(t) \cdot \cos(\phi) \cdot |\delta \cdot X_{best} - X_i|$
    Apply boundary check for X_{new} **if** $ObjFunc(X_{new}) < ObjFunc(X_i)$ **then**
      $X_i = X_{new}$ **if** $ObjFunc(X_i) < ObjFunc(X_{best})$ **then**
        $X_{best} = X_i$
      end
    end
  end
end
return X_{best}

Algorithm 3. Enhanced Sinh Cosh Optimizer with trigonometric operators (I_SCHO) for triple-diode PV models

Results and simulation

This section presents comprehensive experiments that state the effectiveness of the enhanced Sinh Cosh Optimizer with trigonometric Operators(I_ SCHO). The enhanced proposed approach is utilized for the parameter identification of the three PV models for different solar cells. These cells are RTC France cell, Photowatt-PWP201 cell, Kyocera KC200GT - 204.6 W cell, Ultra 85-P cell, and STM6-40/36 module cell. For

Common parameters for all algorithms	
Parameter	**Setting/value**
Population size (N)	30 (for all algorithms) except for I_SCHO (50)
Maximum iterations ($MaxIter$)	500
Algorithm-specific parameters	
Algorithm	Parameter settings
Sinh Cosh Optimizer (I_SCHO)	Exploration weight ($W1$): 0.5 (initially) Exploitation weights ($W2$, $W3$): dynamically adjusted based on iteration number Trigonometric operators coefficients (α, γ): 1 (initially), adjusted with iterations Bounded search strategy parameters ($BS1$, α): $BS1 = 1.55, \alpha = 4.6$ Switching mechanism coefficients (p, q): adjusted to shift focus from exploration to exploitation
Grey Wolf Optimizer (GWO)	Wolves hierarchy: alpha, beta, delta, omega Convergence parameters (a, A, C): $a = 2 \rightarrow 0$, A, C in [−2a, 2a]
Ant Lion Optimizer (ALO)	Random walk parameters: fixed or random step size for ant's walk Exploitation mechanism: Ant lion traps and random walks Selection mechanism: Roulette wheel selection
Sine Cosine Algorithm (SCA)	Trigonometric operators coefficients (α, γ): fixed, adjusted with iterations Exploitation mechanism: cosine and sine functions for local search Selection mechanism: determined by sine and cosine functions
Sooty Tern Optimization Algorithm (STOA)	Exploitation mechanism: guided by the best sooty tern and nearest predator Selection mechanism: determined by distance to the best sooty tern
Tunicate Swarm Algorithm (TSA)	Leadership-based exploration and exploitation
Hunger Games Search (HGS)	Hunger and exploration balance Selection mechanism: leadership and power dynamics
Rat Swarm Optimizer (RSO)	Interaction among rats for exploitation Selection mechanism: determined by fitness and proximity

Table 2. Parameter settings for various optimization algorithms.

each cell, experiment were performed on the three PV models, Single-Diode model (SDM), Double-Diode model (DDM), and Triple-Diode model (TDM).

This section proposes comparative experiments and justifies our recommendation of the proposed optimization algorithm. Results of the I_SCHO are compared with Grey wolf optimizer (GWO)[65], ant lion optimizer (ALO)[54], Sine cosine algorithm (SCA)[66], Sooty Tern Optimization Algorithm (STOA)[67], Tunicate Swarm Algorithm (TSA)[68], Hunger Games Search (HGS)[69], Rat Swarm Optimizer (RSO)[70], and Sinh Cosh Optimizer (SCHO).The parameter settenting for each algorithm can be found in Table 2

Experiments are illustrated in an comprehensive way as follows:

- Experiments on RTC France cell and SDM are shown in Table 3
- Experiments on RTC France cell and DDM are shown in Table 4
- Experiments on RTC France cell and TDM are shown in Table 5
- Experiments on Photowatt-PWP201 cell and SDM are shown in Table 6
- Experiments on Photowatt-PWP201 cell and DDM are shown in Table 7
- Experiments on Photowatt-PWP201 cell and TDM are shown in Table 8
- Experiments on Kyocera KC200GT - 204.6 W cell and SDM are shown in Table 9
- Experiments on Kyocera KC200GT - 204.6 W cell and DDM are shown in Table 10
- Experiments on Kyocera KC200GT - 204.6 W cell and TDM are shown in Table 11
- Experiments on Ultra 85-P cell and SDM are shown in Table 12
- Experiments on Ultra 85-P cell and DDM are shown in Table 13
- Experiments on Ultra 85-P cell and TDM are shown in Table 14
- Experiments on STM6-40/36 module cell and SDM shown in Table 15
- Experiments on STM6-40/36 module cell and DDM shown in Table 16
- Experiments on STM6-40/36 module cell and TDM shown in Table 17The accuracy of P-V and I-V estimation and similarity with the actual measurements are recorded for proving effeciency of estimation. The measured RMSE over 30 trials were measured to the suggested (I_SCHO) in comparision to the state-of-art algorithms. Also the time complexity to reach saturation and minimal RMSE will be represented in the following subsections.

The I_SCHO method and the competing algorithms have been tested using the different datasets in 30 different experiments with 500 iterations in each run to provide a fair benchmarking comparison. We conduct experiments on a machine with the following specifications: 64-bit Windows 10 Professional, 2.40GHz Intel(R) Core(TM) i7-4700MQ processor, and 16GB of RAM. MATLAB R2019a is used for the implementation of each algorithm.

RTC France cell

Experiments on single-diode mode based RTC France cell

In this section, our first experiments were conducted on the SDM-based RTC France cell. Table 3 reports the best-obtained parameters' measurements and the Root Mean Square Error (RMSE). The experimental outcomes were recorded after each optimizer's execution 30 times. The findings reveal that I_SCHO emerges as the optimum algorithm, as inferred from its Best RMSE performance, either comparable to the other algorithms or surpassing them across all performance metrics, as shown in the table.

The convergence curve is employed during our experimental investigations, and the standard deviation is recorded as an auxiliary metric for performance evaluation. I_SCHO algorithm attained stability and minimized Root Mean Square Error (RMSE), as shown in Fig. 4a. I_SCHO consistently outperforms or performs on par with alternative algorithms but never exhibits inferior performance. Furthermore, utilizing the fill factor and Iphoto parameters underscores disparities between the findings yielded by I_SCHO and those produced by the other state-of-the-art algorithms.

Contrary to being the fastest algorithm in achieving convergence, our findings indicate that I_SCHO exhibited a comparable and satisfactory pace relative to the other algorithms. However, it was distinguished that the I_SCHO reached the smallest RMSE value. Notably, this optimal saturation was attained after almost 120 iterations, underscoring the efficacy of I_SCHO in achieving heightened precision within a modest computational timeframe.

The I_SCHO method, compared to the other algorithms, as shown in Fig. 4c, achieved the lowest RMSE among the thirty trials, demonstrating sustainability and great enhancement relative the original SCHO algorithm. Moreover, Fig. 4b and d illustrate the P-V and I-V curves derived from the optimal parameters acquired using the I_SCHO algorithm. These graphical representations demonstrate the congruity between the estimated and the actual measurements. It is observed from these figures that the parameters inferred by I_SCHO facilitate the attainment of current and power levels that exhibit a high degree of consistency with the empirical data.

Experiments on double-diode model-based RTC France cell

This section summarizes the experiments after the thirty trials of the excuted algorithms but now on the DDM-based RTC France. The best and the worst RSME values are again computed, as presented in Table 4. This tabulated data reveals that I_SCHO attains the foremost position concerning the best RMSE which is 0.0016458 among the algorithms surveyed. The worst RMSE and the SD values in Table 4 indicate a notable outperformance of I_SCHO outcomes among 90% of the other algorithms.

Figure 5a measures the convergence curve of the applied algorithms based on DDM. I_SCHO performs better in achieving the lowest Root Mean Square Error (RMSE) than the other algorithms. Despite not being the most rapid, I_SCHO exhibits a satisfactory convergence rate, reaching saturation after approximately 130

	Best-obtained parameters										RMSE				
	I_{ph}(A)	I_{sd}(A)	$R_s(\Omega)$	$R_p(\Omega)$	Non-ideality	I_{sc}(A)	V_{oc}(V)	I_{mp}(A)	V_{mp}(V)	P_{mp}(W)	Best	Worst	SD	Fill factor	Iphoto
GWO	0.7596	0.000000041241	0.0444	39.9736	1.2987	0.7587	0.5736	0.6922	0.453	0.3136	0.0032406	0.067813	0.013456	0.72053	0.76134479
ALO	0.7639	0.000005829	0.01998	89.0681	1.8454	0.7637	0.5736	0.6827	0.448	0.3059	0.0062287	0.073695	0.021761	0.69833	0.76067056
SCA	0.7613	0.000000003651	0.05228	18.3883	1.1355	0.7591	0.5736	0.6871	0.4551	0.3127	0.0066166	0.021788	0.0036783	0.71823	0.76266226
STOA	0.7645	0.000014449	0.01142	100	2	0.7644	0.5736	0.6791	0.448	0.3042	0.0091071	0.021853	0.0045161	0.69385	0.760586869
TSA	0.7614	0.000000468380	0.03426	67.7479	1.5189	0.7609	0.5736	0.6902	0.4507	0.311	0.0017467	0.073707	0.029422	0.71264	0.760884621
HGS	0.7628	0.0000035379	0.02348	100	1.7701	0.7626	0.5736	0.6847	0.4485	0.3071	0.004836	0.073694	0.01981	0.70208	0.76067856214
RSO	0.6845	0.000000001	0.01978	21.3697	1.0692	0.6838	0.5736	0.625	0.4791	0.2994	0.068382	0.23441	0.051381	0.76342	0.761204096
SCHO	0.7929	0.00000004264	0.0937	21.3375	1.3107	0.7894	0.5736	0.704	0.4271	0.3007	0.015603	0.27055	0.049559	0.66406	0.7638397122
I_SCHO	0.762	0.00000046857	0.03478	52.967	1.5196	0.7615	0.5736	0.6891	0.4505	0.3104	0.0012756	0.070287	0.022803	0.71063	0.76099934046

Table 3. Comparison between algorithms based on RTC France cell and SDM.

	Best-obtained parameters												RMSE				
	I_{ph}(A)	I_{sd1}(A)	I_{sd2}(A)	$R_s\,(\Omega)$	$R_p\,(\Omega)$	Non-ideality D1	Non-ideality D2	I_{sc}(A)	V_{oc}(V)	I_{mp}(A)	V_{mp}(A)	P_{mp}(W)	Best	Worst	SD	Fill factor	Iphoto
GWO	0.7626	0.0000000025	0.000004808	0.04172	41.817	1.1359	1.9996	0.7618	0.5736	0.6847	0.4523	0.3097	0.0018936	0.069645	0.020045	0.70868	0.76125882568
ALO	0.7589	0.000000001	0.00000064703	0.0361	176.9716	1.1713	1.5722	0.7587	0.5736	0.6907	0.4503	0.311	0.0017018	0.074296	0.031939	0.71477	0.76065514140
SCA	0.7666	0.000000001975	0.00000019303	0.04369	17.8672	1.1375	1.5025	0.7647	0.5736	0.6838	0.4527	0.3095	0.0057115	0.027575	0.0058651	0.70565	0.762359726
STOA	0.7616	0.000000001353	0.0000027869	0.04371	193.7186	1.1072	1.8652	0.7614	0.5736	0.6915	0.4508	0.3117	0.0026114	0.070345	0.013182	0.71374	0.76067158
TSA	0.7621	0.00000057894	0.0000016383	0.03141	166.042	1.5549	2	0.7619	0.5736	0.6906	0.4498	0.3106	0.0028119	0.070109	0.02951	0.71077	0.76064387764
GS	0.7813	0.00000067569	0.0000049695	0.06595	64.8252	1.6659	1.8624	0.7804	0.5736	0.6873	0.418	0.2873	0.065498	0.3742	0.075451	0.64179	0.76127365437
RSO	0.7225	0.000000001	0.00000016508	0.02776	24.3624	1.3714	1.4211	0.7216	0.5736	0.6491	0.4579	0.2972	0.033309	0.26971	0.068873	0.71813	0.761366487
SCHO	0.7963	0.00000008219	0.00000047184	0.08206	100.6826	1.3895	1.6607	0.7956	0.5736	0.7155	0.4265	0.3052	0.04666	0.21873	0.047397	0.66883	0.76111985166
I_SCHO	0.7603	0.00000010177	0.00000038002	0.03389	48.5335	1.4947	1.5325	0.7598	0.5736	0.6869	0.4509	0.3098	0.0016458	0.070109	0.022708	0.7108	0.76103103363

Table 4. Comparison between algorithms based on RTC France cell and DDM.

	Best-obtained parameters														RMSE				
	I_{ph}(A)	I_{sd1}(A)	I_{sd2}(A)	I_{sd3}(A)	$R_s\,(\Omega)$	$R_p\,(\Omega)$	Non-ideality D1	Non-ideality D2	Non-ideality D3	I_{sc}(A)	V_{oc} (V)	I_{mp} (A)	V_{mp} (A)	P_{mp} (W)	Best	Worst	SD	Fill factor	Iphoto
GWO	0.7592	0.00000008801	0.00000334120	0.00000010615	0.03553	296.7845	1.9232	2	1.4	0.759	0.5736	0.6895	0.4502	0.3105	0.0017827	0.0067064	0.0016413	0.71311	0.760591056
ALO	0.76	0.00000011301	0.00000004885	0.0000053607	0.03336	478.4969	1.8339	1.3515	2	0.7599	0.5736	0.6876	0.4499	0.3094	0.0024381	0.0085795	0.0017563	0.70988	0.76055301715
SCA	0.7605	0.0000019971	0.000000018271	0.000000011969	0.03953	108.7677	1.8645	1.264	1.7077	0.7602	0.5736	0.6912	0.4514	0.312	0.0018542	0.0085337	0.001848	0.71554	0.760776362
STOA	0.7601	0.0000059111	0.000000006288	0.00000000197	0.03774	492.8644	2	1.2	1.7429	0.7599	0.5736	0.6882	0.4508	0.3102	0.0020004	0.0086084	0.0024764	0.71166	0.760558235
TSA	0.7605	0.0000005935	0.000001211	0.00000033937	0.0334	105.4277	2	1.9522	1.5023	0.7602	0.5736	0.6886	0.4499	0.3098	0.0017566	0.0053146	0.0011371	0.71048	0.760740934
HGS	0.7605	0.0000006567	0.00000048421	0.00000000133	0.03365	78.8039	1.9997	1.5291	1.4	0.7601	0.5736	0.6888	0.4503	0.3102	0.0013637	0.0072207	0.0013403	0.71138	0.760824788
RSO	0.7225	0.000000001	0.000000001	0.000000076186	0.03501	23.8375	1.131	1.2	1.4	0.7214	0.5736	0.6519	0.4598	0.2998	0.031562	0.26133	0.067143	0.72445	0.761616819
SCHO	0.7605	0.00000303190	0.0000035438	0.0000069898	0.04711	500	2	2	2	0.7604	0.5736	0.6713	0.4321	0.2901	0.039208	0.10701	0.016283	0.66503	0.76057165461
I_SCHO	0.7603	0.0000004759	0.00000000116	0.00000021014	0.03447	83.0804	1.5244	1.7221	1.873	0.7599	0.5736	0.6895	0.4502	0.3104	0.0012518	0.019984	0.0050127	0.71219	0.760815525

Table 5. Comparison between algorithms based on RTC France cell and TDM.

	Best-obtained parameters										RMSE				
	I_{ph}(A)	I_{sd}(A)	$R_s(\Omega)$	$R_p(\Omega)$	Non-ideality	I_{sc}(A)	V_{oc}(V)	I_{mp}(A)	V_{mp}(V)	P_{mp}(W)	Best	Worst	SD	Fill factor	Iphoto
GWO	1.028	0.0000034	1.215	1395.46	1.35	1.0288	16.78	0.9126	12.649	11.5429	0.00248	0.09515	0.041022	0.67105	1.0325985
ALO	1.0276	0.0000052	1.1626	2444.5348	1.3951	1.027	16.7783	0.9138	12.6409	11.551	0.002849	0.10909	0.050648	0.67038	1.032190678
SCA	1.04	0.000014063	1.05392	3212.7428	1.5166	1.0395	16.7783	0.9178	12.5712	11.5381	0.0084218	0.095373	0.029376	0.66152	1.032038
STOA	1.031	0.0000080576	1.08484	3371.3807	1.4457	1.0305	16.7783	0.9151	12.6319	11.5594	0.0046288	0.095158	0.042769	0.66855	1.03203198
TSA	1.0321	0.0000062632	1.08619	1046.1691	1.4173	1.0309	16.7783	0.9112	12.6689	11.5442	0.0039485	0.095156	0.042848	0.66739	1.032771167
HGS	1.0322	0.0000026138	1.23522	766.2768	1.3213	1.0304	16.7783	0.9127	12.6675	11.5618	0.0020424	0.095154	0.041414	0.66873	1.0333630761208
RSO	0.9798	0.0000013707	1.55726	1549.7809	1.2567	0.9787	16.7783	0.8743	12.4996	10.9280	0.047137	0.21667	0.035113	0.6655	1.032736681
SCHO	1.0305	0.0000089043	1.09381	1771.5268	1.4593	1.0298	16.7783	0.9107	12.6164	11.4899	0.0039	0.10151	0.034465	0.66502	1.0323370113902
I_ SCHO	1.0321	0.000002774	1.22821	791.0461	1.3274	1.0304	16.7783	0.9127	12.6657	11.5595	0.0020526	0.0085558	0.0010026	0.66866	1.033301863577090

Table 6. Comparison between algorithms based on Photowatt-PWP201 cell and SDM.

	Best-obtained parameters												RMSE				
	I_{ph}(A)	I_{sd1}(A)	I_{sd2}(A)	$R_s\,(\Omega)$	$R_p\,(\Omega)$	Non-ideality D1	Non-ideality D2	I_{sc}(A)	V_{oc}(V)	I_{mp}(A)	V_{mp}(V)	P_{mp}(W)	Best	Worst	SD	Fill factor	Iphoto
GWO	1.0247	0.0000011775	0.0000032734	1.20533	7936.9214	1.3085	1.4227	1.0244	16.7778	0.916	12.6468	11.5839	0.0034197	0.093977	0.043337	0.67398	1.0318567
ALO	1.029	0.000001433	0.0000018894	1.25173	1187.2724	1.2834	1.4659	1.0278	16.7778	0.9146	12.6612	11.5795	0.0024325	0.10757	0.042366	0.67151	1.032788
SCA	1.0212	0.00000003624	0.00000096756	1.34227	7184.9787	1.2065	1.2308	1.0209	16.7778	0.9218	12.7152	11.7214	0.0078876	0.094336	0.024284	0.68431	1.03189273893
STOA	1.033	0.000000001027	0.00000069131	1.38582	536.0132	1	1.2	1.0302	16.7778	0.9146	12.7062	11.6213	0.0034659	0.093976	0.015475	0.67235	1.034367386
TSA	1.0248	0.0000039224	0.0000046481	1.16068	4340.0418	1.3677	1.9232	1.0244	16.7778	0.9137	12.6702	11.5774	0.0043982	0.093995	0.02206	0.67362	1.031975912
HGS	1.0609	0.000000095094	0.00000065881	58.93204	5168.5398	1.2653	1.9136	0.9641	16.7778	0.8614	12.3912	10.6743	0.12202	0.27083	0.032278	0.65991	1.043463513
RSO	0.9801	0.000000001	0.00000065712	1.25296	6672.3643	1	1.2	0.9798	16.7778	0.8889	12.8772	11.4471	0.029347	0.15892	0.023766	0.69633	1.031893737
SCHO	1.0317	0.00000099102	0.0000027265	1.19911	968.5094	1.3032	1.3901	1.0303	16.7778	0.9133	12.6594	11.5623	0.0023598	0.10565	0.031668	0.66888	1.032977348
I_SCHO	1.0322	0.000000001	0.0000026482	1.23384	771.2225	1.1689	1.3228	1.0304	16.7778	0.9127	12.6666	11.5613	0.0020441	0.0033266	0.00042216	0.66873	1.0333505715

Table 7. Comparison between algorithms based on Photowatt-PWP201 cell and DDM.

	Best-obtained parameters														RMSE				
	I_{ph}(A)	I_{sd1}(A)	I_{sd2}(A)	I_{sd3}(A)	$R_s\,(\Omega)$	$R_p\,(\Omega)$	Non-ideality D1	Non-ideality D2	Non-ideality D3	I_{sc} (A)	V_{oc} (V)	I_{mp} (A)	V_{mp} (V)	P_{mp} (W)	Best	Worst	SD	Fill factor	Iphoto
GWO	1.0296	0.00000000115	0.0000019436	0.0000053504	1.14084	1555.379	1.8051	1.9249	1.4	1.0287	16.7778	0.9123	12.645	11.5356	0.0027902	0.0041604	0.00035922	0.66834	1.03245673388
ALO	1.03	0.000001685	0.0000011185	0.000005193	1.19834	1289.4483	1.7132	1.2742	1.5571	1.0289	16.7778	0.9124	12.654	11.546	0.0024813	0.0057872	0.0007181	0.66883	1.03265880664
SCA	1.0317	0.00000014596	0.00000000421	0.0000053696	1.14039	1070.2204	2	1.6376	1.4	1.0305	16.7778	0.9116	12.6558	11.5375	0.003307	0.010902	0.0020777	0.66733	1.03279934229
STOA	1.0297	0.00000002872	0.00000011595	0.0000053711	1.14199	1362.8212	1.7364	1.5805	1.4	1.0287	16.7778	0.912	12.6504	11.537	0.0027851	0.0083507	0.0013224	0.66843	1.032564524
TSA	1.0294	0.0000035334	0.000003074	0.0000023431	1.15192	1743.5092	1.5841	1.363	1.693	1.0285	16.7778	0.9116	12.6324	11.5159	0.0031319	0.0051007	0.00050869	0.66733	1.032381633
HGS	1.0317	0.000000001	0.000002346	0.0000035738	1.23767	823.5174	1.2921	1.312	2	1.03	16.7778	0.9127	12.6684	11.5619	0.0020893	0.0047412	0.00065069	0.66904	1.033250554
RSO	1.0213	0.0000063474	0.0000026244	0.0000075829	1.17375	3305.5794	1.4907	1.5744	1.604	1.0208	16.7778	0.8985	12.5064	11.2375	0.017224	0.083632	0.017177	0.65612	1.032066338
SCHO	1.0292	0.00000084919	0.0000021583	0.00000092793	1.20215	1556.0881	1.3568	1.35	1.4154	1.0283	16.7778	0.9146	12.645	11.5655	0.0027702	0.0068163	0.00097018	0.67039	1.032497034
I_SCHO	1.0317	0.0000025196	0.000000003913	0.000000013566	1.23988	791.9172	1.3179	1.3686	1.4001	1.03	16.7778	0.9129	12.6684	11.5651	0.0020514	0.0036206	0.00036658	0.66926	1.033315303685

Table 8. Comparison between algorithms based on Photowatt-PWP201 cell and TDM.

	Best-obtained parameters										RMSE				
	I_{ph}(A)	I_{sd}(A)	$R_s(\Omega)$	$R_p(\Omega)$	Non-ideality	I_{sc}(A)	V_{oc}(V)	I_{mp}(A)	V_{mp}(V)	P_{mp}(W)	Best	Worst	SD	Fill factor	Iphoto
GWO	8.2278	0.00001682	0.04444	2409.0816	1.8187	8.1884	32.8998	7.4619	26.5947	198.4475	0.13802	0.46175	0.12392	0.73664	8.21015145650641
ALO	8.078	0.000000001	0.2571	4633.776	1.0465	8.039	32.8998	7.5931	26.9703	204.7872	0.049784	0.47463	0.11362	0.7743	8.21045551655129
SCA	8.178	0.000021976	0.02054	1432.8822	1.8578	8.1389	32.8998	7.403	26.6695	197.4334	0.15558	0.20595	0.042769	0.73733	8.21011769662512
STOA	8.4721	0.000000001022	0.24779	52.277	1.0479	8.3919	32.8998	7.4757	26.9546	201.5053	0.097551	0.23672	0.028192	0.72985	8.24891480968098
TSA	8.2442	0.000016784	0.04519	1754.6195	1.8195	8.2047	32.8998	7.4733	26.6085	198.8523	0.14066	0.46527	0.14014	0.73667	8.21021144453805
HGS	7.8322	0.00000031919	155.78079	4034.7927	1.9583	7.4352	32.8998	6.5951	24.1226	159.0915	1.4407	4.4166	0.83009	0.65037	8.52698288959642
RSO	7.389	0.000000001	0.18002	1425.6271	1.0554	7.3528	32.8998	6.9501	27.7131	192.6089	0.5393	2.7504	0.74923	0.7962	8.211036696
SCHO	8.097	0.000000001931	0.24689	699.4284	1.0775	8.0556	32.8998	7.5685	26.9533	203.9967	0.042772	0.56218	0.15469	0.76972	8.21289802359947
I_SCHO	8.2011	0.000000001	0.24811	142.5823	1.0469	8.1478	32.8998	7.5345	27.0113	203.5173	0.028211	0.12365	0.016921	0.75922	8.22428638348108

Table 9. Comparison between algorithms based on Kyocera KC200GT - 204.6 W cell and SDM.

	Best-obtained parameters												RMSE				
	I_{ph}(A)	I_{sd1}(A)	I_{sd2}(A)	$R_s\,(\Omega)$	$R_p\,(\Omega)$	Non-ideality D1	Non-ideality D2	I_{sc}(A)	V_{oc}(V)	I_{mp}(A)	V_{mp}(A)	P_{mp}(W)	Best	Worst	SD	Fill factor	Iphoto
GWO	8.1097	0.00000000143	0.0000044195	0.23252	8687.4096	1.0674	1.9744	8.0708	32.8995	7.5529	26.919	203.3155	0.043489	0.46992	0.15999	0.76571	8.21021974365
ALO	8.1536	0.0000004246	0.0000007107	0.14966	10026.301	1.4231	1.9913	8.1145	32.8995	7.5279	26.7516	201.3841	0.073239	0.59766	0.14759	0.75435	8.21012254813
SCA	8.3295	0.00000000286	0.000002049	0.20926	85.3434	1.0991	2	8.2695	32.8995	7.4964	27.0486	202.7679	0.071443	0.18257	0.015475	0.7453	8.23013028427
STOA	8.1525	0.000000001	0.0000021554	0.23963	285.481	1.0493	1.9225	8.1068	32.8995	7.5352	26.9595	203.1439	0.035954	0.48418	0.078423	0.76167	8.216891279
TSA	8.2108	0.0000013382	0.0000021991	0.12325	17318.0651	1.53	1.9898	8.1716	32.8995	7.5375	26.6706	201.0298	0.094735	0.46872	0.15658	0.74777	8.21005843
HGS	8.2368	0.00000049721	0.00000081927	3.92473	3340.1579	1.7954	1.93	7.9572	32.8995	5.0872	26.7759	136.2137	1.8297	4.8188	0.72285	0.52032	8.219646866
RSO	7.7995	0.000000001	0.000000044849	0.054	583.7381	1.0331	1.3867	7.7616	32.8995	7.3084	27.6588	202.1423	1.0388	3.7453	0.74938	0.79162	8.210759484
SCHO	8.1033	0.000000007015	0.00000061455	0.21455	10377.3755	1.1489	1.7043	8.0645	32.8995	7.5517	26.8947	203.1006	0.04716	0.43847	0.10678	0.7655	8.210169737
I_SCHO	8.2011	0.000000001	0.000000001	0.24811	142.5975	1.0469	2.0	8.1478	32.8995	7.5347	27.0108	203.5172	0.028212	0.086105	0.01845	0.75923	8.2242846817

Table 10. Comparison between algorithms based on Kyocera KC200GT - 204.6 W cell and DDM.

	Best-obtained parameters														RMSE			Fill factor	Iphoto
	I_{ph}(A)	I_{sd1}(A)	I_{sd2}(A)	I_{sd3}(A)	$R_s\,(\Omega)$	$R_p\,(\Omega)$	Non-ideality D1	Non-ideality D2	Non-ideality D3	I_{sc} (A)	V_{oc} (V)	I_{mp} (A)	V_{mp} (V)	P_{mp} (W)	Best	Worst	SD		
GWO	8.1442	0.00000000252	0.00000012872	0.00000064779	0.17841	4397.1724	1.4991	1.3296	1.9347	8.105	32.8995	7.5452	26.7759	202.0294	0.061146	0.1215	0.014362	0.75766	8.21033310188
ALO	8.1514	0.00000007885	0.0000047945	0.000000001	0.16473	2680.9808	1.3012	1.9555	1.4483	8.112	32.8995	7.523	26.8002	201.6179	0.067612	0.14957	0.017278	0.75546	8.21050445081
SCA	8.21	0.00000004315	0.00000000565	0.00000000123	0.19272	209.2731	1.2529	1.7004	1.4	8.1633	32.8995	7.5289	26.8623	202.2446	0.051378	0.12174	0.014148	0.75304	8.21756072482
STOA	8.21	0.000000001166	0.000000018602	0.000000073109	0.20708	187.0912	1.7668	1.2	2	8.1618	32.8995	7.5325	26.8947	202.583	0.044006	0.1526	0.028402	0.75444	8.219087301
TSA	8.1331	0.00000087969	0.00000012321	0.0000021031	0.16181	5182.8616	2	1.3284	2	8.094	32.8995	7.524	26.8272	201.8488	0.06636	0.12014	0.012796	0.75801	8.21025632
HGS	8.2008	0.000000001	0.0000015422	0.000000001036	0.24284	158.6512	1.048	2	2	8.1492	32.8995	7.5311	26.9946	203.3001	0.030525	0.10598	0.01821	0.75828	8.222566511
RSO	7.7995	0.000000001	0.000000001	0.00000024548	0.11505	1311.5828	1.1347	1.2	1.4	7.7616	32.8995	7.2252	27.1728	196.3277	0.24629	1.1736	0.23247	0.76885	8.210720159
SCHO	8.1022	0.0000032872	0.000000041675	0.000000001063	0.17903	17906.4095	1.9743	1.2545	1.8931	8.0635	32.8995	7.5148	26.8704	201.9267	0.060831	0.13202	0.018222	0.76117	8.210082085
I_SCHO	8.1988	0.000000001001	0.000000001	0.000000013566	0.24608	147.3436	1.0486	1.2224	1.9991	8.1461	32.8995	7.5346	27.0054	203.4744	0.028597	0.072663	0.012483	0.75922	8.223711551234

Table 11. Comparison between algorithms based on Kyocera KC200GT - 204.6 W cell and TDM.

	Best-obtained parameters										RMSE			Fill factor	Iphoto
	I_{ph}(A)	I_{sd}(A)	$R_s\,(\Omega)$	$R_p\,(\Omega)$	Non-ideality	I_{sc}(A)	V_{oc}(V)	I_{mp}(A)	V_{mp}(V)	P_{mp}(W)	Best	Worst	SD		
GWO	5.1621	0.0000092805	0.42042	1008.0389	1.5539	5.1593	22.1999	4.6039	15.1024	69.5292	0.019988	0.15173	0.020057	0.60705	5.4522729959752
ALO	5.2624	0.0000029822	0.43611	84.9474	1.4332	5.2349	22.1999	4.5793	15.1727	69.4813	0.010494	0.18583	0.052562	0.59787	5.47797994044396
SCA	5.1958	0.0000032206	0.46304	509.0351	1.4365	5.1904	22.1999	4.6474	15.044	69.9177	0.044178	0.31704	0.028192	0.60678	5.45495755477432
STOA	5.4065	0.000000005453	0.57552	36.727	1	5.3225	22.1999	4.5834	15.2789	70.0290	0.049987	0.17284	0.043814	0.59267	5.53540311539403
TSA	5.1666	0.000021076	0.37937	2794.1675	1.654	5.1652	22.1999	4.5935	15.1144	69.4280	0.016823	0.16638	0.033971	0.60547	5.45073995760002
HGS	5.7225	0.0000002084	9.17169	3600	1.3819	5.1058	22.1999	4.6455	15.2195	70.7020	0.12367	1.6018	0.39294	0.62376	8.52698288959642
RSO	4.905	0.000000006357	0.4674	405.5023	1	4.8988	22.1999	4.5288	15.6382	70.8231	0.18333	1.3383	0.21192	0.6512	5.456281854
SCHO	5.1793	0.000026487	0.36533	635.2921	1.6859	5.1756	22.1999	4.5821	15.1337	69.3441	0.012603	0.15979	0.038888	0.60352	5.45313409152468
I_SCHO	5.2408	0.0000048828	0.4232	106.8719	1.4835	5.2195	22.1999	4.5811	15.1596	69.4472	0.0064055	0.12358	0.042705	0.59934	5.47158136366189

Table 12. Comparison between algorithms based on Ultra 85-P cell and SDM.

	Best-obtained parameters												RMSE				
	I_{ph}(A)	I_{sd1}(A)	I_{sd2}(A)	$R_s(\Omega)$	$R_p(\Omega)$	Non-ideality D1	Non-ideality D2	I_{sc}(A)	V_{oc}(V)	I_{mp}(A)	V_{mp}(A)	P_{mp}(W)	Best	Worst	SD	Fill factor	Iphoto
GWO	5.2047	0.00000000108	0.00000017776	0.53033	122.4786	1.1663	1.2	5.1816	22.1994	4.6328	15.1488	70.1818	0.036762	0.15601	0.023038	0.61012	5.47359843126
ALO	5.3314	0.00000001246	0.00000029577	0.50579	52.5983	1.1022	1.2661	5.2799	22.1994	4.5871	15.21	69.7703	0.028494	0.15938	0.026065	0.59525	5.50240725244
SCA	5.1775	0.0000000012	0.00000054618	0.52899	189.278	1.0	1.3035	5.1624	22.1994	4.6317	15.1362	70.1066	0.037715	0.13821	0.036612	0.61173	5.46523162613
STOA	5.1775	0.000000002982	0.0000046296	0.4296	234.0348	1.1089	1.484	5.1674	22.1994	4.5993	15.1758	69.7987	0.021901	0.13106	0.033069	0.60847	5.460004237
TSA	5.1775	0.0000044525	0.000005	0.43706	6540.0321	1.5201	1.6075	5.1765	22.1994	4.625	15.0624	69.6632	0.028616	0.1595	0.01911	0.60621	5.450364213
HGS	5.464	0.00000039669	0.00000078128	75.0408	12297.4304	1.7395	1.94	5.3374	22.1994	4.6782	14.6754	68.6543	0.30254	1.6358	0.34911	0.57943	5.483256732
RSO	5.1775	0.000000001	0.00000012022	0.61672	525.4003	1	1.2	5.1708	22.1994	4.6956	15.0588	70.710	0.09443	1.098	0.22799	0.616	5.456397278
SCHO	5.1775	0.000000001	0.00000014817	0.55384	130.2823	1	1.2	5.155	22.1994	4.6197	15.1146	69.8242	0.048411	0.12723	0.022518	0.61015	5.473168305
I_ SCHO	5.245	0.000000001	0.0000041299	0.43621	101.1935	1.0507	1.4728	5.2219	22.1994	4.5829	15.1632	69.4909	0.0082285	0.095215	0.036567	0.59946	5.4734928629

Table 13. Comparison between algorithms based on Ultra 85-P cell and DDM.

	Best-obtained parameters														RMSE				
	I_{ph}(A)	I_{sd1}(A)	I_{sd2}(A)	I_{sd3}(A)	$R_s(\Omega)$	$R_p(\Omega)$	Non-ideality D1	Non-ideality D2	Non-ideality D3	I_{sc} (A)	V_{oc} (V)	I_{mp} (A)	V_{mp} (V)	P_{mp} (W)	Best	Worst	SD	Fill factor	Iphoto
GWO	5.1796	0.00000987	0.000007792	0.0000019146	0.38393	472.473	1.6189	1.7106	1.608	5.1747	22.1994	4.5845	15.1254	69.3428	0.011519	0.04023	0.006665	0.60363	5.45442867831
ALO	5.2324	0.0000030781	0.0000010829	0.0000050764	0.40968	123.5033	1.7607	1.604	1.5045	5.2144	22.1994	4.5785	15.1542	69.383	0.0035317	0.0464	0.0086512	0.59939	5.46807857906
SCA	5.1775	0.00000000726	0.00001	0.000000001	0.40013	280.943	2	1.5621	1.4	5.1695	22.1994	4.5854	15.1488	69.4626	0.014485	0.062453	0.011604	0.60529	5.45776201741
STOA	5.1775	0.000009882	0.0000099912	0.000000001091	0.40236	17852.2786	1.7721	1.5901	1.6271	5.1767	22.1994	4.6086	15.0858	69.525	0.02108	0.053492	0.011661	0.60499	5.450122833
TSA	5.1876	0.0000045129	0.000005807	0.0000082609	0.38698	344.7795	1.7625	1.6032	1.6302	5.1811	22.1994	4.5834	15.1326	69.3586	0.011709	0.035523	0.0046747	0.60303	5.45611713
HGS	5.2264	0.00001	0.0000052136	0.00001	0.40332	141.1851	2	1.5025	1.9995	5.2109	22.1994	4.5761	15.1524	69.3394	0.0024466	0.014743	0.0019511	0.59942	5.465568748
RSO	5.1775	0.000000001	0.000000001	0.0000017967	0.44281	119.3206	1	1.2	1.4	5.1577	22.1994	4.5749	15.2748	69.8811	0.040316	0.35231	0.073528	0.61032	5.470225581
SCHO	5.1838	0.0000013873	0.0000091284	0.000006953	0.3907	311.0823	1.6808	1.7753	1.5518	5.1766	22.1994	4.5834	15.1434	69.4082	0.01103	0.039251	0.0066635	0.60398	5.456844881
I_SCHO	5.226	0.0000045547	0.0000058162	0.0000096185	0.4015	141.8065	1.4972	2.0	1.8157	5.2106	22.1994	4.5758	15.1524	69.3338	0.0024582	0.011586	0.0016567	0.5994	5.465430697469

Table 14. Comparison between algorithms based on Ultra 85-P cell and TDM.

	Best-obtained parameters										RMSE				
	I_{ph}(A)	I_{sd}(A)	$R_s\,(\Omega)$	$R_p\,(\Omega)$	Non-ideality	I_{sc}(A)	V_{oc}(V)	I_{mp}(A)	V_{mp}(V)	P_{mp}(W)	Best	Worst	SD	Fill factor	Iphoto
GWO	1.6563	0.0000079427	0.00008	3226.0159	1.7073	1.6561	21.0199	1.4995	16.9337	25.3915	0.0050662	0.079431	0.024613	0.7294	1.66300004048811
ALO	1.6598	0.0000044431	0.04554	987.669	1.63	1.6596	21.0199	1.4988	16.9729	25.4383	0.0029415	0.0279	0.0068089	0.72922	1.66307667982106
SCA	1.6589	0.0000060301	0.00012	921.7588	1.6707	1.6587	21.0199	1.4943	16.9726	25.3624	0.0043911	0.026298	0.0053974	0.72741	1.66300022078316
STOA	1.6492	0.0000050102	0.00004	3484.313	1.6457	1.649	21.0199	1.4989	17.0167	25.5066	0.0069348	0.03941	0.0091463	0.73586	1.663000017281450
TSA	1.6698	0.0000018326	0.1599	468.547	1.5266	1.669	21.0199	1.4987	16.9686	25.4309	0.0035231	0.079443	0.034134	0.72488	1.66356753405435
HGS	1.6649	0.0000037776	0.05443	647.7796	1.6108	1.6646	21.0199	1.4974	16.9835	25.4315	0.0027755	0.07943	0.022104	0.72685	1.663139734851890
RSO	1.4967	0.000000001	0.25187	1046.1333	1	1.4962	21.0199	1.4	17.946	25.1251	0.13234	0.20671	0.031118	0.7989	1.663400384
SCHO	1.6595	0.0000060142	0.00004	1006.348	1.671	1.6593	21.0199	1.4962	16.9832	25.4096	0.0042032	0.062237	0.021475	0.72851	1.66300007080054
I_ SCHO	1.662	0.0000037583	0.05965	762.1551	1.61	1.6617	21.0199	1.498	16.9808	25.4379	0.002506	0.011506	0.0020548	0.72828	1.66313014813878

Table 15. Comparison between algorithms based on STM6-40/36 module cell and SDM.

	Best-obtained parameters												RMSE				
	I_{ph}(A)	I_{sd1}(A)	I_{sd2}(A)	$R_s\,(\Omega)$	$R_p\,(\Omega)$	Non-ideality D1	Non-ideality D2	I_{sc}(A)	V_{oc}(V)	I_{mp}(A)	V_{mp}(A)	P_{mp} (W)	Best	Worst	SD	Fill factor	Iphoto
GWO	1.6617	0.00000000123	0.0000047807	0.15624	865.6216	1.0723	1.6726	1.6612	21.0186	1.499	16.9812	25.4547	0.0024958	0.021524	0.0038653	0.72902	1.66330015813
ALO	1.6642	0.000000001	0.0000028518	0.20072	601.2134	1.0624	1.6063	1.6635	21.0186	1.4985	16.992	25.4624	0.0017693	0.084096	0.018923	1.66355520378	324.13058
SCA	1.6556	0.0000000022	0.0000035241	0.10328	2198.0991	1.4579	1.6012	1.6554	21.0186	1.5042	16.9452	25.4892	0.004812	0.030909	0.0058039	0.73257	1.66307813935
STOA	1.6763	0.000000001004	0.0000039278	0.48315	306.8788	1	1.799	1.6735	21.0186	1.497	17.073	25.5581	0.0075698	0.028879	0.0046207	0.72662	1.66561823
TSA	1.6556	0.00000037446	0.0000048371	0.07621	16241.9622	1.6065	1.6535	1.6555	21.0186	1.5059	16.9128	25.469	0.006649	0.076332	0.031443	0.73196	1.663007803
HGS	1.7055	0.00000016545	0.0000011868	1.78456	9247.6267	1.2596	1.7815	1.705	21.0186	1.5348	14.643	22.4739	0.27225	0.88644	0.15237	0.62713	1.663320917
RSO	1.5798	0.000000001	0.000000011161	0.036	1020.9597	1	1.2	1.5796	21.0186	1.4748	17.892	26.3867	0.071359	0.1348	0.023482	0.79474	1.663058639
SCHO	1.6625	0.000000073214	0.0000032528	0.11182	709.8519	1.3702	1.6187	1.662	21.0186	1.4988	16.9758	25.443	0.0022913	0.041194	0.011952	0.72832	1.663261973
I_SCHO	1.6638	0.000000001	0.000003132	0.25739	614.9374	1.0419	1.6356	1.663	21.0186	1.4988	16.9956	25.473	0.0016782	0.0030151	0.00025951	0.66873	1.6636960599

Table 16. Comparison between algorithms based on STM6-40/36 module cell and DDM.

	Best-obtained parameters														RMSE			Fill factor	Iphoto
	I_{ph}(A)	I_{sd1}(A)	I_{sd2}(A)	I_{sd3}(A)	R_s(Ω)	R_p(Ω)	Non-ideality D1	Non-ideality D2	Non-ideality D3	I_{sc} (A)	V_{oc} (V)	I_{mp} (A)	V_{mp} (A)	P_{mp} (W)	Best	Worst	SD		
GWO	1.663	0.0000051009	0.00000002168	0.0000014089	0.22698	650.8576	1.9273	1.2046	1.6077	1.6623	21.0186	1.4986	16.9974	25.4721	0.0017108	0.008463	0.0016875	0.72906	1.66357995263
ALO	1.663	0.000000001	0.0000039506	0.00000020182	0.32925	643.5973	1.0239	1.7089	1.6151	1.662	21.0186	1.4989	17.0028	25.4849	0.0018006	0.013612	0.0021425	0.72954	1.66385075161
SCA	1.663	0.00000000116	0.00000000617	0.0000034561	0.05909	739.1331	1.4117	1.9139	1.6002	1.6627	21.0186	1.4992	16.9992	25.486	0.0032949	0.012922	0.0022143	0.72926	1.66313294648
STOA	1.663	0.0000049306	0.00000000119	0.00000045298	0.21562	560.4434	1.9638	1.2094	1.4	1.6622	21.0186	1.4992	17.0028	25.4902	0.0021123	0.011001	0.0023471	0.7296	1.663639816
TSA	1.663	0.0000021954	0.0000017322	0.00000040914	0.19121	592.4858	1.7578	2	1.4	1.6623	21.0186	1.4992	16.9938	25.4774	0.0018098	0.0077131	0.0015907	0.72919	1.663536681
HGS	1.663	0.000000001	0.000001456	0.0000029771	0.13975	639.4063	1.3929	1.508	2	1.6625	21.0186	1.4991	16.9866	25.4643	0.0017901	0.0039511	0.00053731	0.72874	1.663363463
RSO	1.6462	0.00000193	0.0000017708	0.0000020343	0.36445	9717.7181	1.8407	1.6197	1.6332	1.646	21.0186	1.4903	16.5942	24.7311	0.038259	0.10336	0.018684	0.71485	1.663062369
SCHO	1.6555	0.0000041195	0.0000020634	0.000000001	0.06641	1841.4156	1.8481	1.5646	1.428	1.6553	21.0186	1.501	16.9668	25.467	0.0040225	0.011939	0.0017802	0.73198	1.663059974
I_ SCHO	1.663	0.000000001034	0.000000001567	0.0000024523	0.18511	626.5283	1.0898	1.2	1.5813	1.6623	21.0186	1.4992	16.9884	25.4696	0.0017386	0.0033737	0.00048366	0.72895	1.663491346489

Table 17. Comparison between algorithms based on STM6-40/36 module cell and TDM.

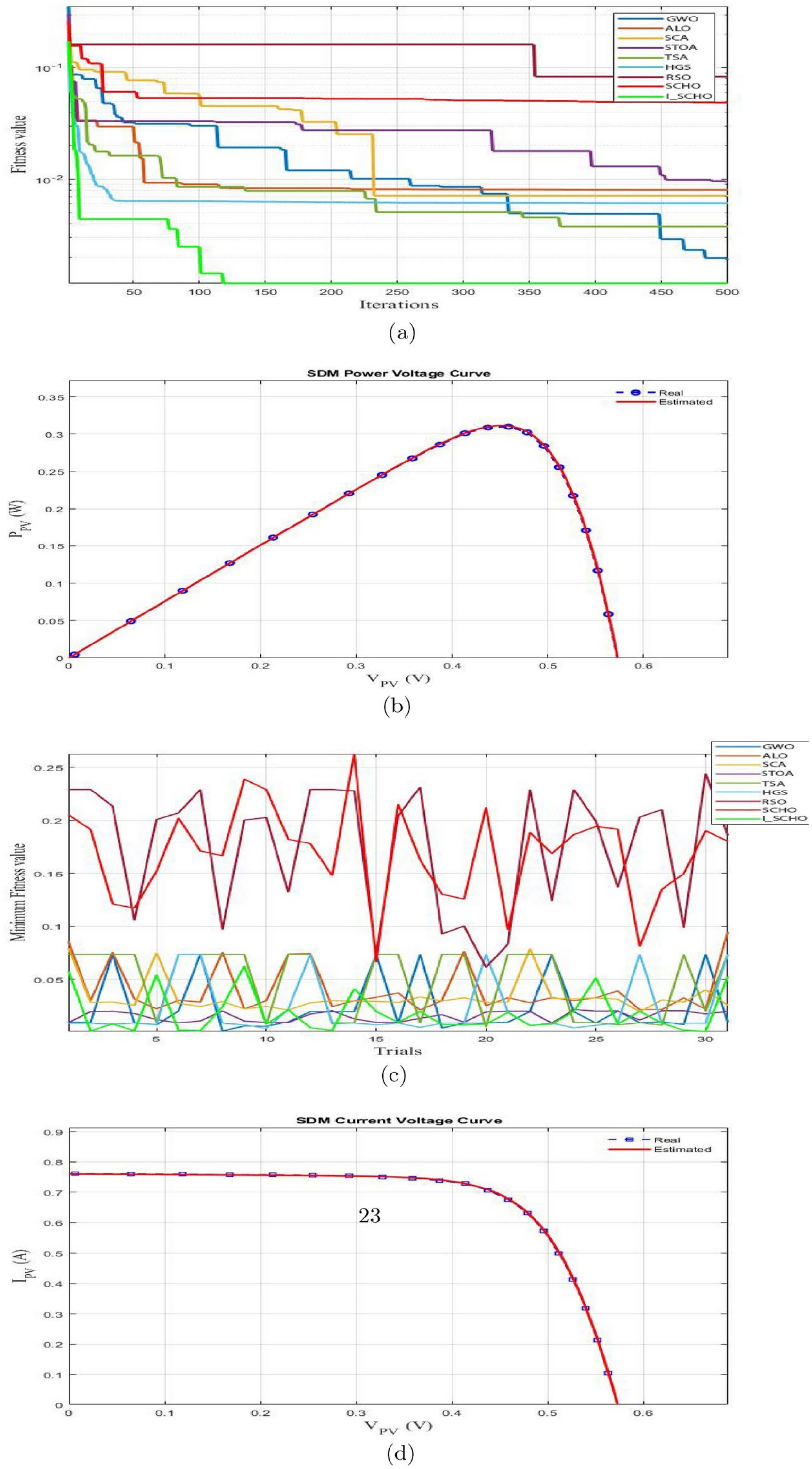

Fig. 4. Comparison between algorithms based on SDM and RTC France cell.

iterations. This convergence behavior is notably compensated by its ability to achieve the lowest RMSE values consistently.

Although the I_SCHO approach produced the lowest RMSE out of thirty trials, indicating sustainability due to the lack of oscillations in the recorded RMSE values, it is very comparable to GWO and STOA algorithms, as shown in Fig. 5c. This minimum fitness function value is reflected on the P-V and I-V curves that show high identity between the estimated and the Real measured values as indicated in Fig. 5b and d.

Experiments on triple-diode model-based RTC France cell

In this section, we apply the I_SCHO algorithm to identify the optimal parameters based on TDM and RTC France cell, thus facilitating a comprehensive evaluation of its performance. Table 5 presents the outcomes yielded by various algorithms in this context, clearly indicating that I_SCHO acts as the best-performing algorithm. Additionally, the table includes the RMSE values contrasting I_SCHO's results with those of its competitors, illustrating notable distinctions between I_SCHO and all other algorithms examined. The best RMSE achieved was 0.0012518, the minimum achieved RMSE for all the algorithms. The worst RMSE recorded in the 30 trials of I_SCHO was 0.019984, which is also the most optimum relative to the other algorithms. Although the measured SD wasn't the minimum, it was 0.0050127, which is very comparable to the different competitive algorithms.

Furthermore, Fig. 6a depicts the convergence curves of each algorithm, underscoring the superiority of I_SCHO in achieving the optimum RMSE. Analysis of this figure reveals that I_SCHO achieves the lowest RMSE after approximately 120 iterations. As Fig. 6c illustrates, I_SCHO represents an enhanced version of SCHO, demonstrating superior performance by achieving lower RMSE (Root Mean Square Error) values. However, it is essential to note that these improved results were attained with increased computation time, indicating a higher complexity for I_SCHO. Despite this, compared with other algorithms that attained similar RMSE values, like SCA, HGS, and TSA, I_SCHO is faster and achieves the best optimum RMSE among the considered methods. I_SCHO emerges as the most accurate among the algorithms compared to estimate the unknown parameters of the TDM-based RTC France solar cell, as evidenced by Fig. 6b and d. These figures demonstrate a high level of consistency between the I-V and P-V curves estimated by I_SCHO and the corresponding measured data, as stated before in experiments of SDM and DDM- based RTC cell.

Photowatt-PWP201

Experiments on single-diode model (SDM)-based Photowatt-PWP201

To emphasize the conclusions from Table 3, other experiments were recorded in Table 6, presenting the measurements, but now on the SDM-based Photowatt-PWP201 cell.

After executing the optimizer 30 times, the experiments state that I_SCHO is the best algorithm based on the computed best and worst RMSE values which were 0.0020526 and 0.0085558 respectively, in addition to achieving the minimum SD to be 0.0010026 .The experiments yielded the lowest RMSE and standard deviation (SD) while maintaining the Fill Factor and Iphoto values, outperforming other state-of-the-art algorithms. This demonstrates the efficiency of the applied algorithm.

Figure 7a shows the convergence curve where the smallest RMSE value is achieved after around 60 iterations by I_SCHO. These experiments again emphasize the efficiency of I_SCHO in achieving high precision within a very small duration achieving very satisfactory number of trials compared to other algorithms, especially the original SCHO algorithm.

Figure 7b and d illustrate the P-V and I-V curves derived from the optimal parameters obtained using the I_SCHO algorithm on the SDM-based Photowatt-PWP201 cell. These graphs serve as a testament to the I_SCHO algorithm's reliability, demonstrating the high alignment between the estimated and actual measurements. The parameters inferred by I_SCHO enable the attainment of current and power levels that closely match the empirical data, providing reassurance about the algorithm's reliability.

The I_SCHO approach produced the lowest RMSE out of thirty trials, indicating that no oscillations were made to achieve the minimum RMSE, Fig. 7c shows that that I_SCHO is the most sustainable and outperforms all the other algorithms .

Experiments on double-diode model (DDM)-based Photowatt-PWP201

This section presents the results of experiments conducted by executing our proposed modified algorithm thirty times on the DDM-based Photowatt-PWP201 cell. Table 7 shows the best-measured parameters, which yield the lowest RMSE values and represent optimal fitness. It is indicated that the best and worst RMSE, 0.0020441 and 0.0033266, respectively, are very close. This approach between the measured RMSE values states the stability of the I_SCHO algorithm regarding the measuring fitness function. This table indicates that I_SCHO significantly outperforms nearly all other algorithms, which is clear evidence of its effectiveness.

Figure 8a depicts the convergence curves of the evaluated competitive algorithms, demonstrating that I_SCHO consistently achieves the lowest Root Mean Square Error (RMSE) within a satisfactory time frame. I_SCHO reaches saturation after approximately 110 iterations, closely approximating the performance of the SCHO algorithm, which saturates in 100 iterations but with a higher RMSE value. Figure 8b and d illustrate that the readings between the measured and estimated values are nearly identical between the P-V and I-V characteristics. Additionally, Fig. 8c again demonstrates that the RMSE remains consistently stable and minimal across the 30 different trials.

Experiments on triple-diode model (TDM)-based Photowatt-PWP201

Experiments were also conducted to find the ideal measured parameters for the TDM and Photowatt-PWP201 cell. The results recorded by the different algorithms are shown in Table 8, which unequivocally shows that I_SCHO is the best-performing method based on the RMSE and SD measurements. Along with comparing

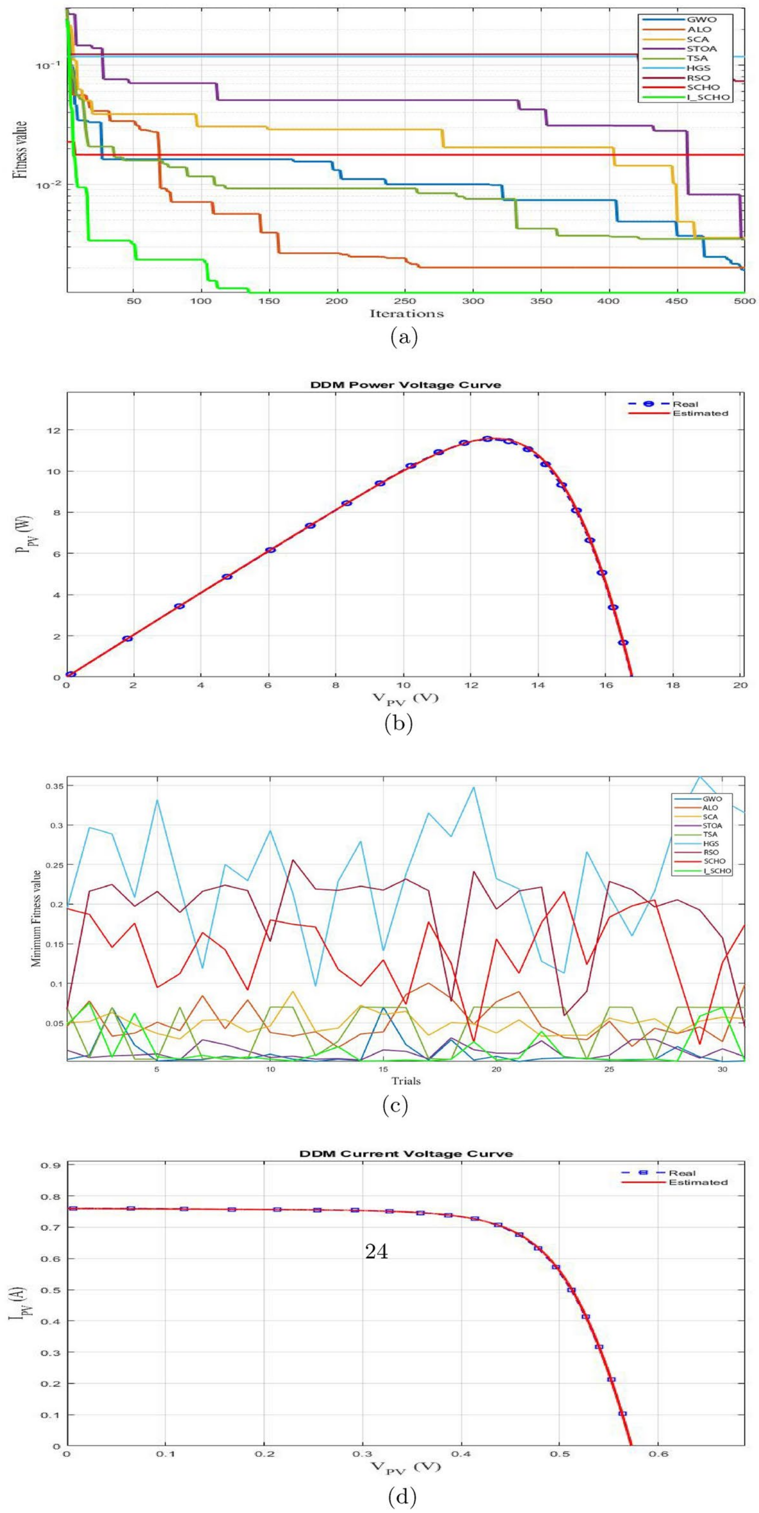

Fig. 5. Comparison between algorithms based on DDM and RTC France cell.

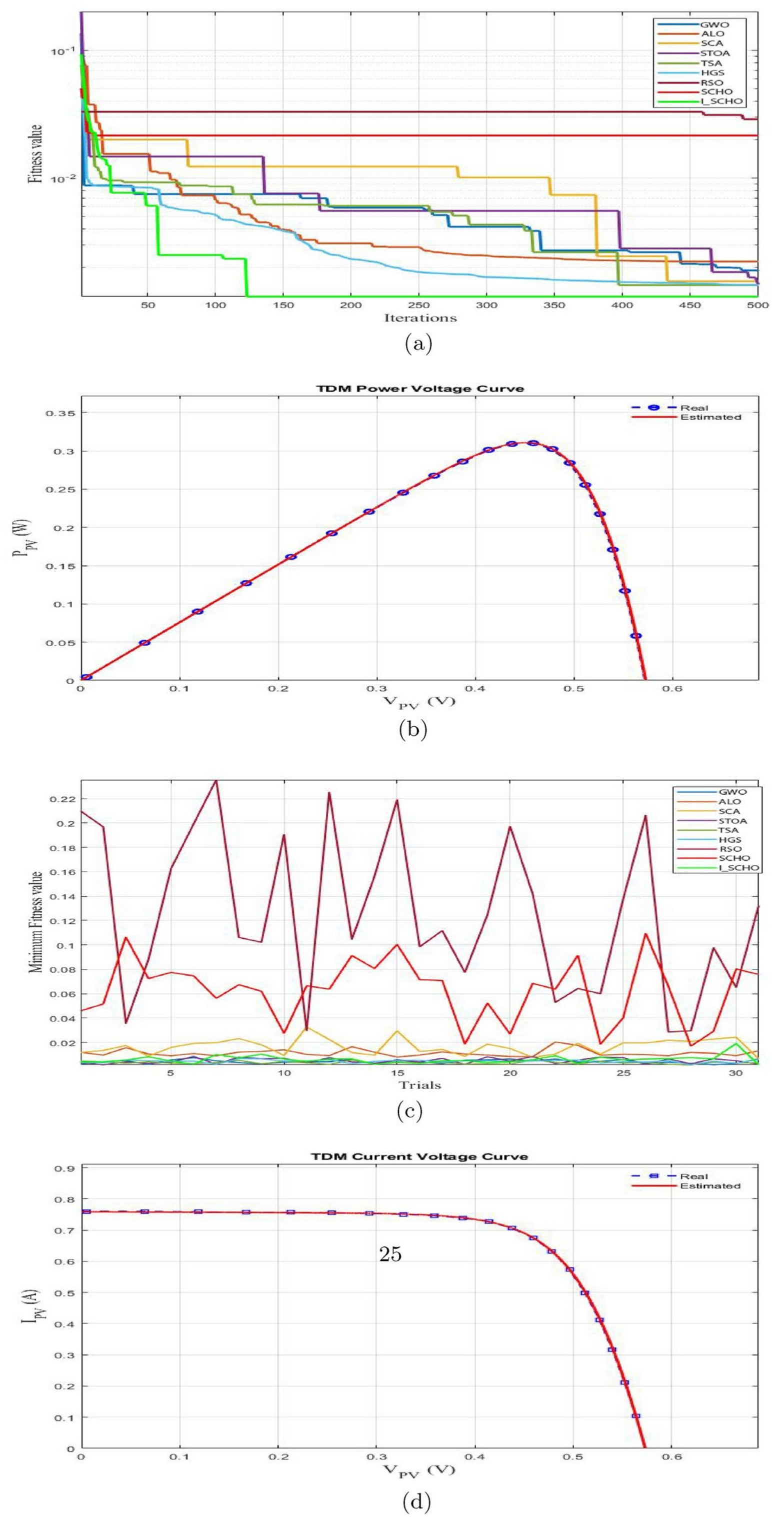

Fig. 6. Comparison between algorithms based on TDM and RTC France cell.

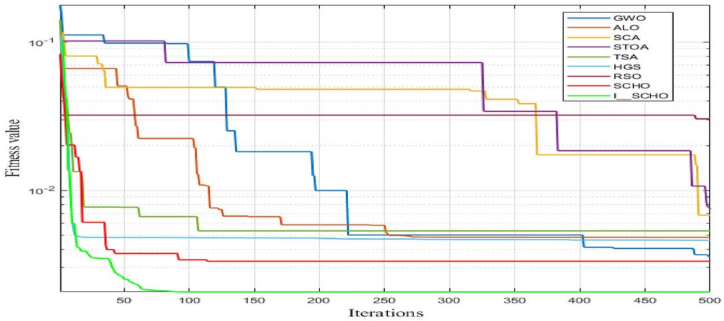

(a)

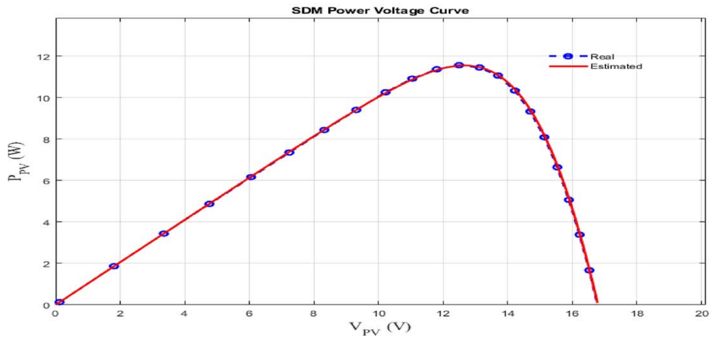

(b)

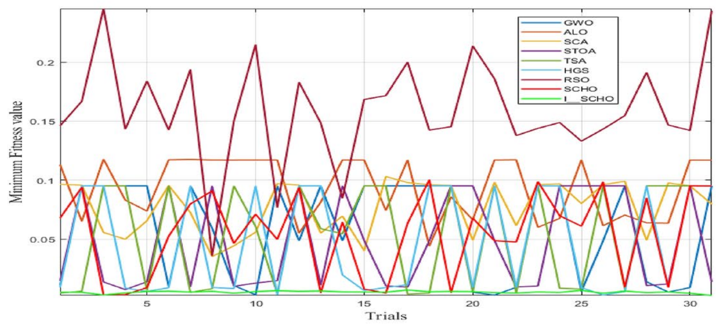

(c)

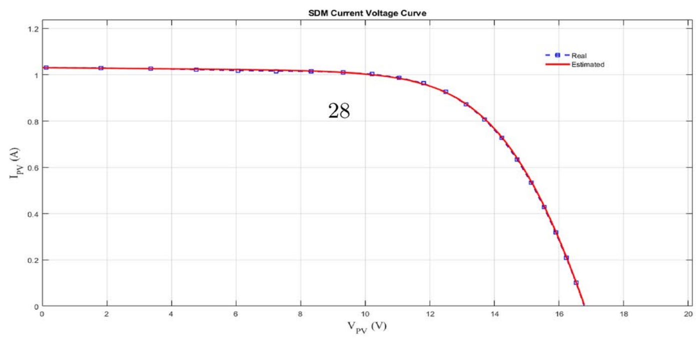

(d)

Fig. 7. Comparison between algorithms based on SDM and Photowatt-PWP201 cell.

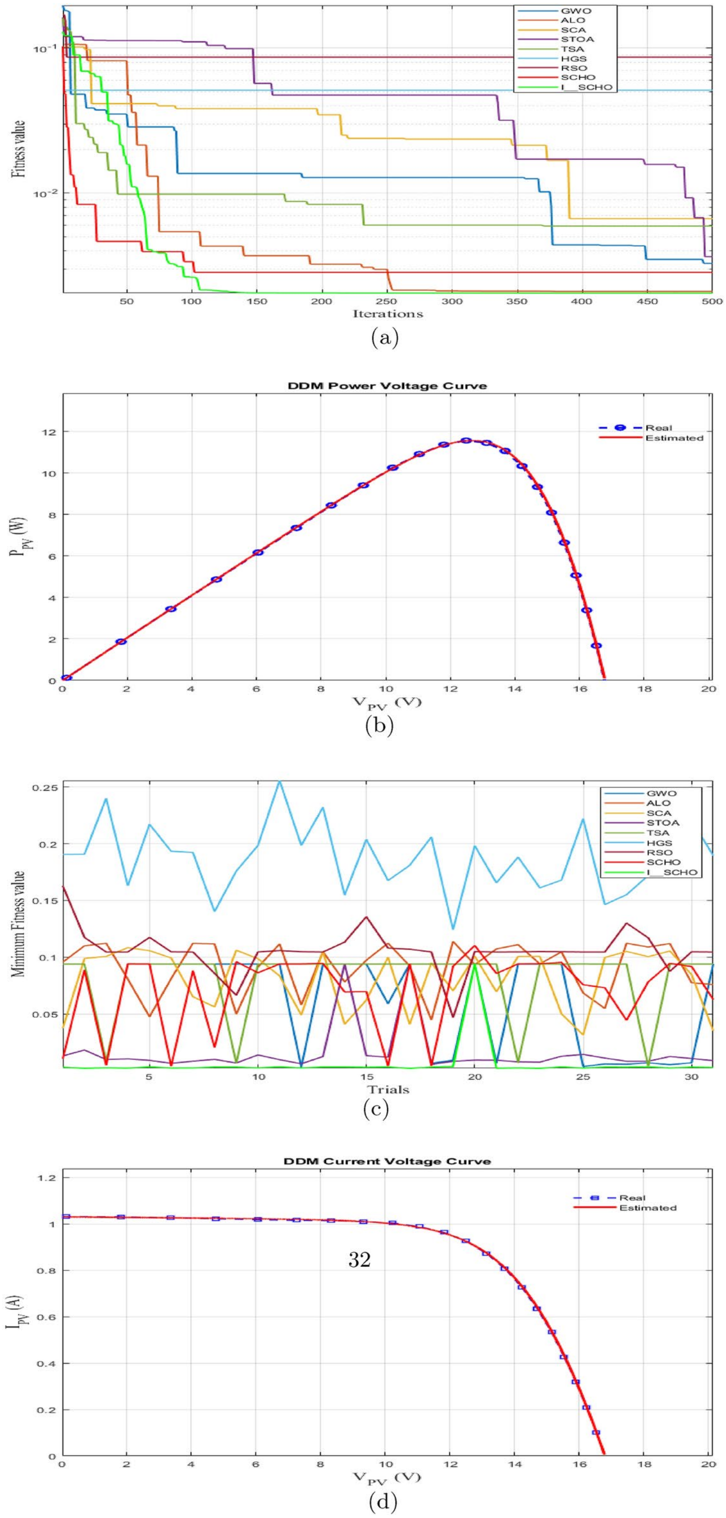

Fig. 8. Comparison between algorithms based on DDM and Photowatt-PWP201 cell.

I_SCHO's outcomes to its rivals, the table emphasises the critical distinctions between I_SCHO and the other algorithms examined. The best RMSE value is 0.0020514, and the worst RMSE value is 0.0036206. On the other side, regarding the SD, the most optimum value is 0.00036658 and is achieved by our suggested enhanced I_SCHO algorithm. Figure 9a shows the convergence curves for each algorithm, highlighting I_SCHO's outperformance. Analysis of this figure shows that after about 170 iterations, I_SCHO achieves the lowest RMSE, proving the most accuracy for estimating unknown parameters. The I_SCHO algorithm reaches saturation after approximately 170 iterations, closely matching the time performance of the TSA and, on the other side, achieving an RMSE value comparable to the GWO algorithm, which saturates after 500 iterations but with a higher RMSE value. Figure 9b and d illustrate that the readings between the observed and estimated values for the P-V and I-V characteristics are nearly identical. Additionally, Fig. 9c indicates that the RMSE remains consistently low and stable across 30 trials, and very comparable to HGS, SCHO, STOA, and TSA.

Kyocera KC200GT - 204.6 W

Experiments on single-diode model (SDM)-based Kyocera KC200GT - 204.6 W

Table 9 presents the root mean square error (RMSE) and the optimal parameter values from experiments conducted with 30 iterations of each optimizer on the Kyocera KC200GT - 204.6 W cell and SDM. Table 9 displays the outcomes, revealing that the I_SCHO algorithm exhibits superior performance based on its best RMSE, worst RMSE and SD. The implemented algorithm performs noticeably better than the other competitive algorithms by obtaining the minimum Root Mean Square Error (RMSE) as the fitness function which is 0.028211. The worst RMSE is 0.12365 and this is the minimum among all the other algorithms.

In our experimental analysis, we utilized convergence curves as shown in Fig. 10a. The I_SCHO algorithm demonstrated stability and effectively minimized the RMSE although with high time complexity after 360 iterations. On the other side, Fig. 10b and d prove high consistency between the measured actual values and the estimated values. This robust performance instil confidence in the algorithm's capabilities that indicates high convergence between the estimated and the measured P-V and I-V characteristics. Figure 10c states the robustness of I_SCHO algorithm by achieving the least RMSE during the different 30 trials with small deviation from the mean computed RMSE.

Experiments on double-diode model (DDM)-based Kyocera KC200GT - 204.6 W

This section presents the results of our proposed modified algorithm thirty times on the DDM-based Kyocera KC200GT - 204.6 W. Table 10 outlines the best-measured parameters of I_SCHO algorithms, demonstrating optimal fitness by achieving the lowest RMSE values. The data in the Table states that the effectiveness of I_SCHO achieves the minimal best and worst RMSE and the minimal SD, showcasing a substantial improvement over nearly all other algorithms.

Figure 11a states that number of trials required for saturation of the DDM-based Kyocera KC200GT-204.6 W experiments was much less than that of the SDM. Comparing the estimated and measured P-V and I-V characteristics, high alignment was recorded, as shown in Fig. 11b and d. The measured RMSE showed persistence towards minimal, as shown in Fig. 11c.

Experiments on triple-diode model (TDM)-based Kyocera KC200GT - 204.6 W

To comprehensively evaluate the performance of the I_SCHO algorithm, tests were conducted to determine the optimal measured parameters for the TDM and Photowatt-PWP201 cell. Table 11, based on RMSE measurements, clearly demonstrates that I_SCHO is the best-performing method among all the algorithms tested. The table highlights the key differences between I_SCHO and the other algorithms by comparing their RMSE values. The I_SCHO algorithm achieved 0.0285 best RMSE and 0.072 worst RMSE. Additionally, Fig. 12a illustrates the convergence curves for each method, emphasizing the outperformance of I_SCHO in achieving the lowest RMSE after 370 iterations.

According to Fig. 12a, the experiments conducted using the TDM-based Kyocera KC200GT-204.6 W exhibited significantly lower temporal complexity compared to STOA, ALO, GWO, and TSA. A high degree of alignment was observed when contrasting the estimated and measured P-V and I-V characteristics, as illustrated in Fig. 12b and d. Furthermore, Fig. 12c shows that the measured RMSE consistently approached a minimum value, indicating a stable and reliable performance during the 30 trials, which was comparable to HGS and STOA algorithms.

Ultra 85-P

Experiments on single-diode model (SDM)-based ultra 85-P cell

This section summarizes the measured optimal parameter values and root mean square error (RMSE), as presented in Table 12. These results were derived from experiments conducted using the Ultra 85-P cell and SDM, after running the optimizer 30 iterations. The recorded results reveals that the I_SCHO method outperforms others based on best RMSE which is 0.0064055, worst RMSE which is 0.12358, and standard deviation (SD) which is 0.042705. The proposed applied method satisfies the optimum fitness function.

The enhanced I_SCHO applied algorithm significantly surpass the other competitive algorithms and as depicted in Fig. 13a, convergence curves show very comparable time complexity, where saturation occurs after 180 iteration, in addition to demonstrating stability and the minimized RMSE relative to SCHO, RSO, GWO, and TSA, as it was observed that these competitive algorithms achieved comparable performance to I_SHCO, although I_SHCO was still better and outperforming. Fig. 13c highlights the comparability of the I_SCHO algorithm with the other algorithms but achieving the lowest RMSE across the thirty trials.

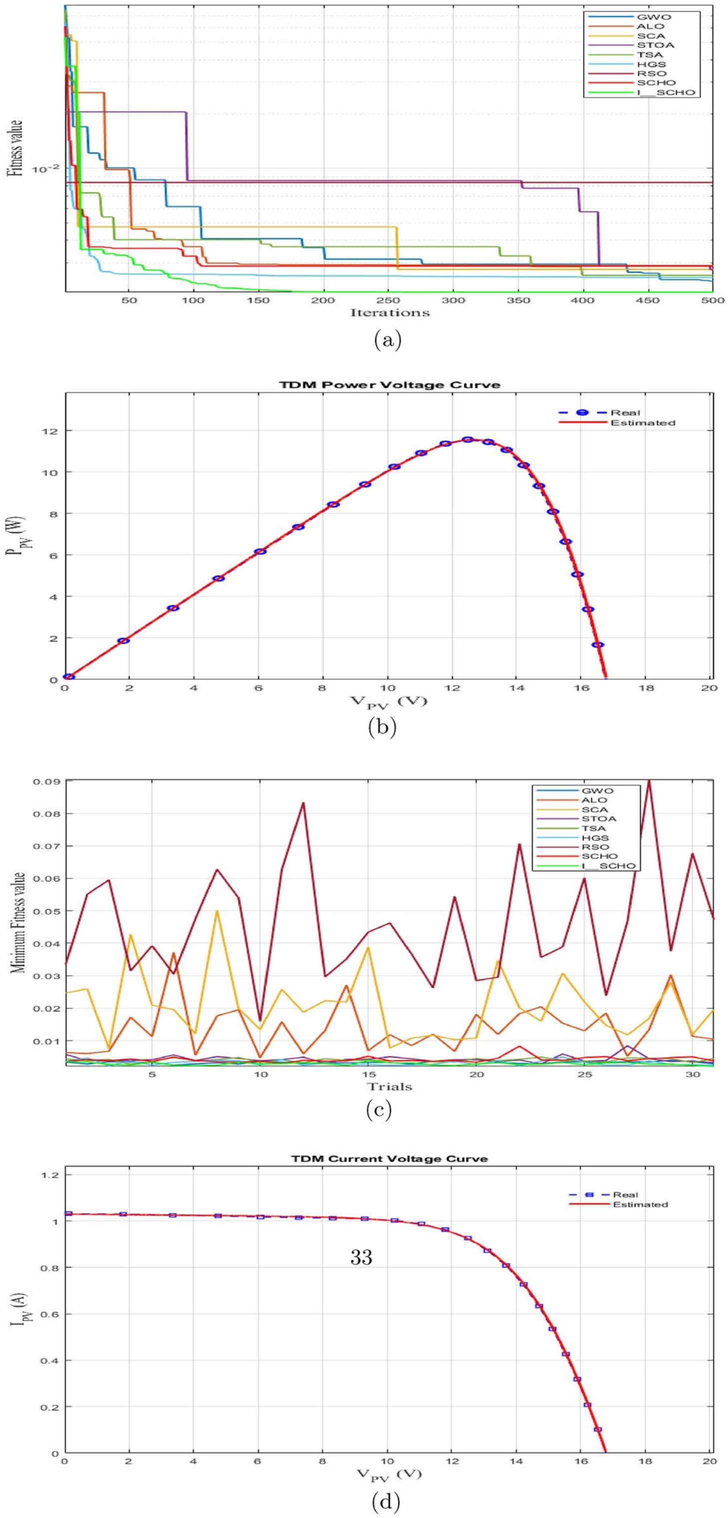

Fig. 9. Comparison between algorithms based on TDM and Photowatt-PWP201 cell.

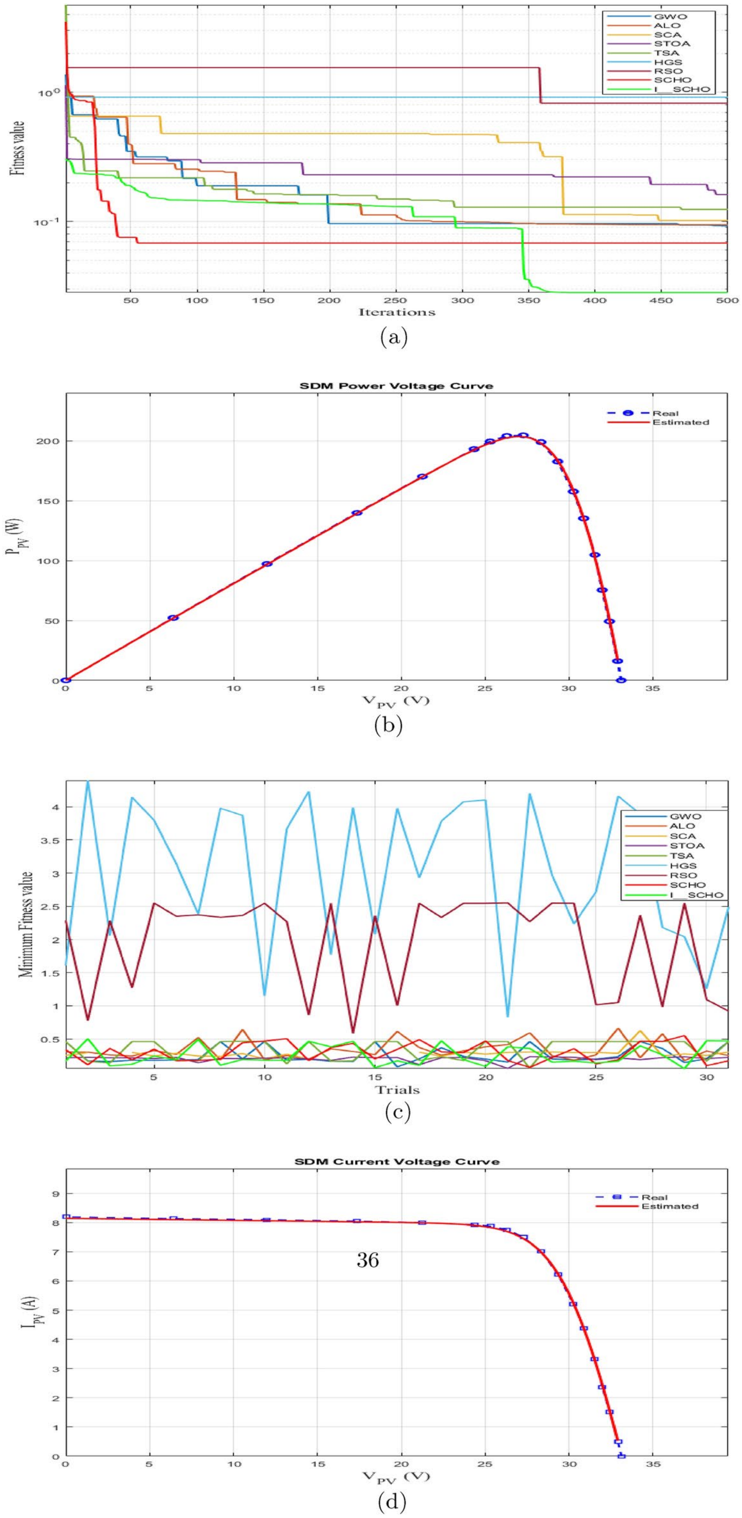

Fig. 10. Comparison between algorithms based on SDM and Kyocera KC200GT - 204.6 W cell.

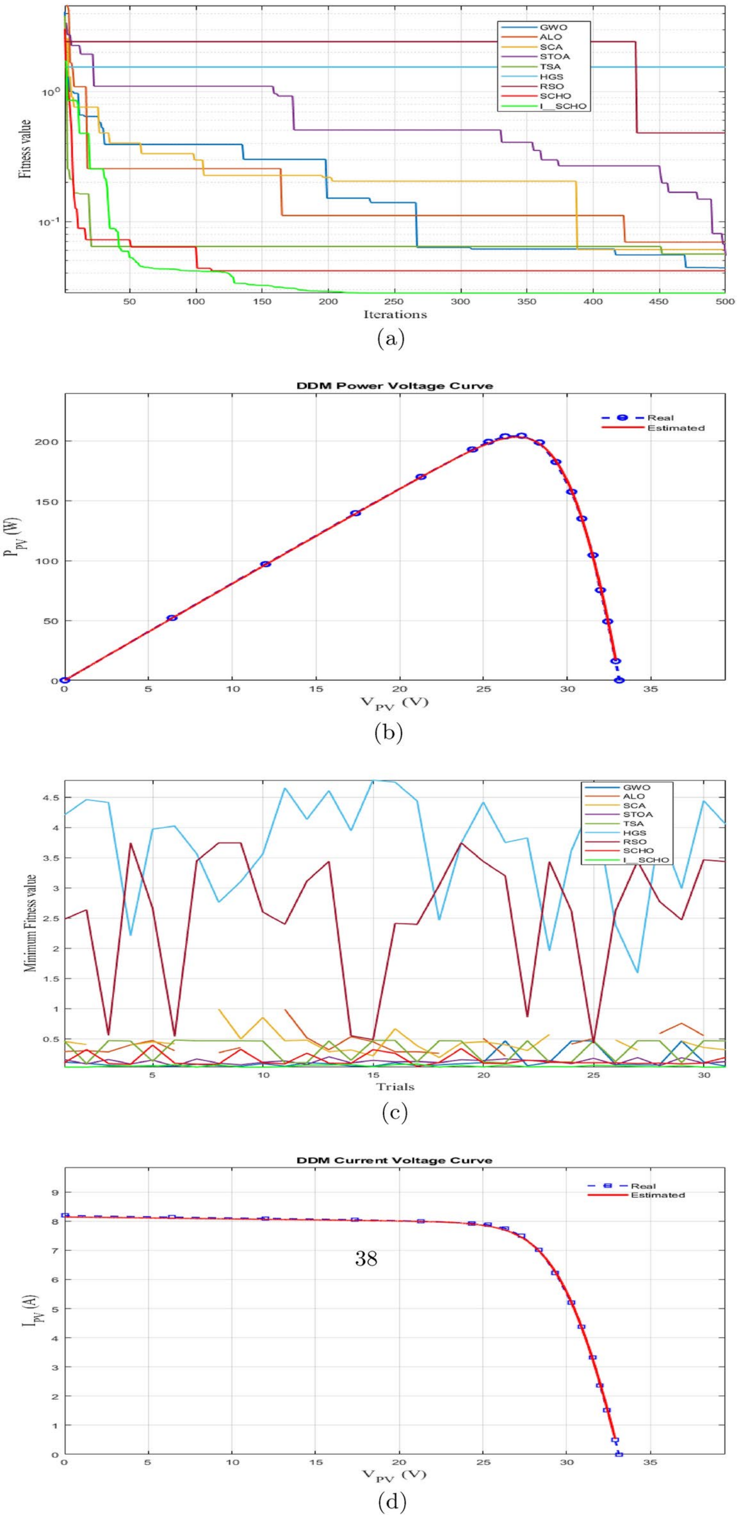

Fig. 11. Comparison between algorithms based on DDM and Kyocera KC200GT - 204.6 W cell.

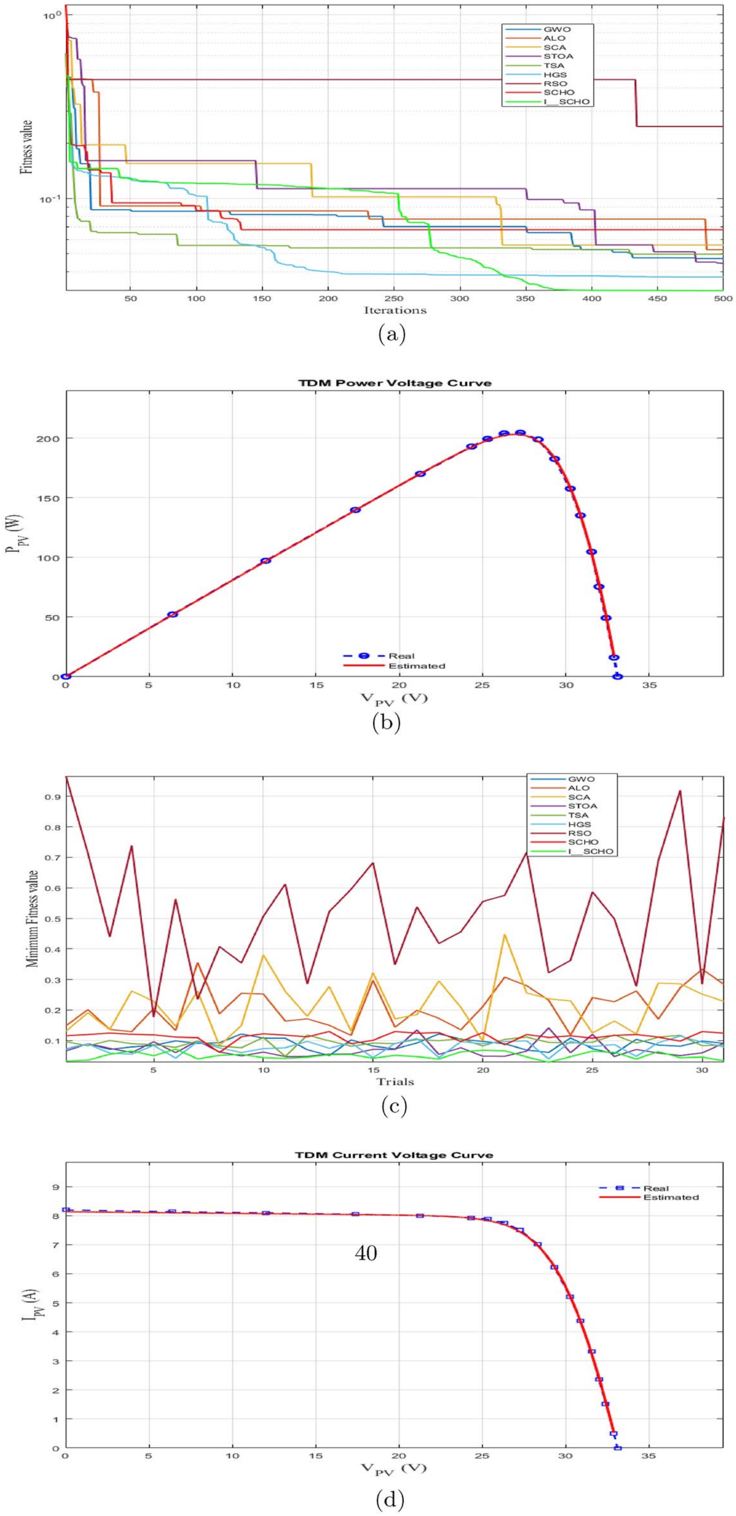

Fig. 12. Comparison between algorithms based on TDM and Kyocera KC200GT - 204.6 W cell.

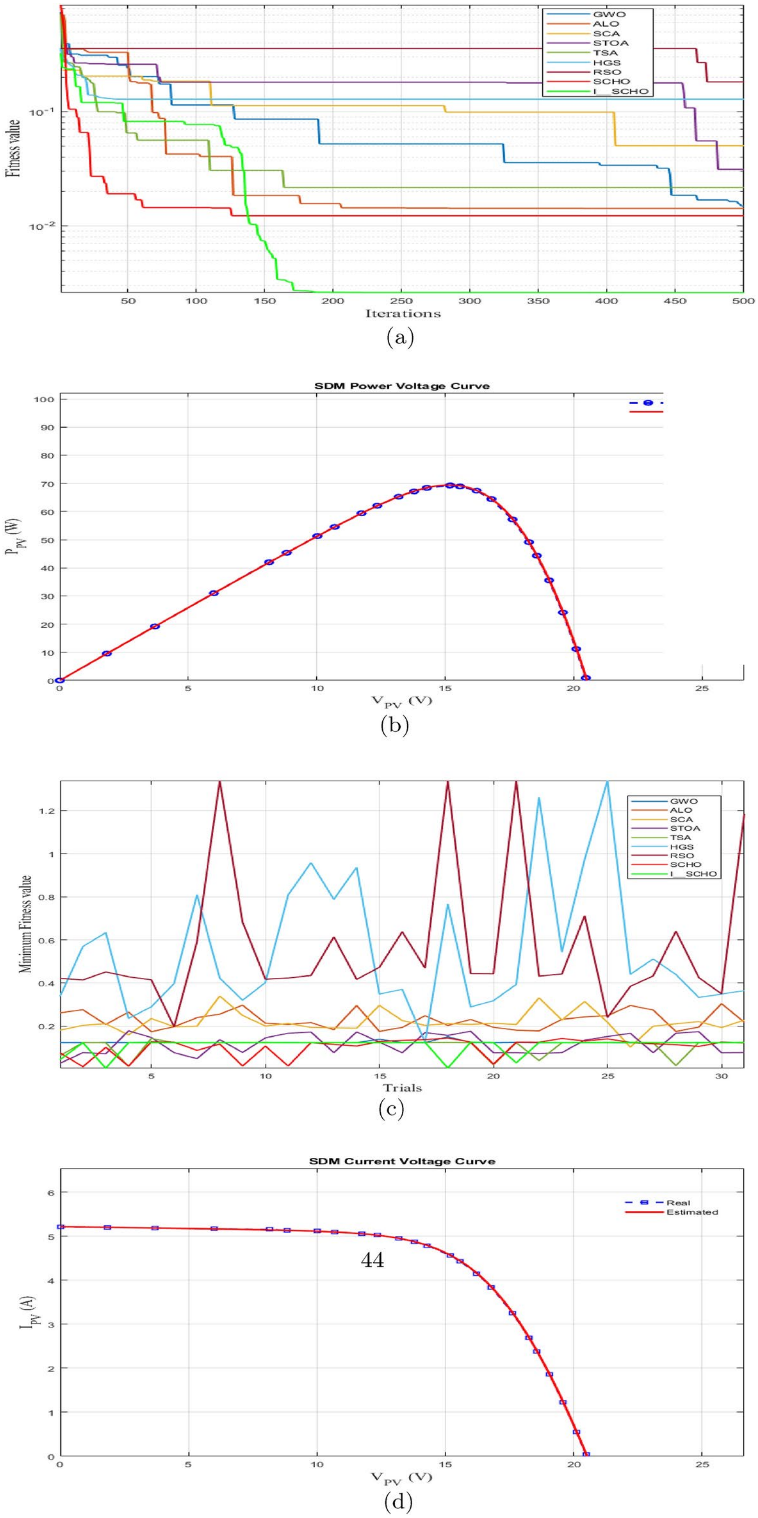

Fig. 13. Comparison between algorithms based on SDM and ultra 85-P W cell.

Figure 13b and d further illustrate a high degree of consistency between the estimated and measured values. The accurate performance, as evidenced by Fig. 13b and d, which display strong convergence between the estimated and measured P-V and I-V characteristics, should instill confidence in the algorithm's capabilities.

Experiments on double-diode model (DDM)-based ultra 85-P cell

This section presents the results of applying our proposed modified method on the DDM-based Ultra 85-P. Table 13 displays the optimal parameters, as indicated by the data in Table 13 that the I_SCHO algorithm achieves the lowest best RMSE 0.0082285, the least worst RMSE value 0.095215, and a comparable standard deviation (SD), indicating a significant improvement over nearly all other methods.

Figure 14a shows that the DDM-based Ultra 85-P trials exhibited significantly higher time complexity than the SDM-based Ultra 85-P experiments, where saturation time is doubled and the least RMSE is reached after around 400 trials. The time analysis of the other best performing algorithms, like TSA, ALO, and STOA, also saturate after large number of trials. Figure 14b and d illustrate high alignment between the measured and estimated P-V and I-V characteristics. Additionally, the observed RMSE values, as depicted in Fig. 14c, consistently approached the minimum, demonstrating the method's robustness during all the 30 trials.

Experiments on triple-diode model (TDM)-based ultra 85-P

To fully assess the I_SCHO algorithm's performance on Ultra 85-P cell, tests were carried out to identify the ideal measured parameters using the TDM model. Table 14 presents the results of different algorithms and shows that, according to RMSE measurements, I_SCHO is the best-performing approach. The table illustrates the improved performance of I_SCHO over the other algorithms by comparing the RMSE values, which were comparable in terms of worst RMSE and standard deviation (SD) and highly near to those of the HGS algorithm in terms of the best RMSE.

The convergence curves for each method are shown in Fig 15a, which emphasises the outperformance of I_SCHO in achieving the least RMSE values. This figure's analysis indicates that I_SCHO attains the lowest RMSE after about 300 iterations, roughly matching the HGS algorithm's performance which converges after 160 iterations.

The I_SCHO algorithm exhibits higher temporal complexity than HGS but demonstrated stability and effectively achieves very comparable RMSE values, which outperforms all the other algorithms. Notably, as shown in Fig. 15c, it consistently achieved the lowest RMSE across all the 30 trials, underscoring the durability of the I_SCHO algorithm. This robustness is further highlighted by the strong convergence between the estimated and measured P-V and I-V characteristics, as depicted in Fig. 15b and d, emphasizing the algorithm's reliability.

STM6-40/36 module

Experiments on single-diode model (SDM)-based STM6-40/36 module

Table 15 presents the root mean square error (RMSE) and the optimal parameter values derived from experiments conducted with 30 iterations of each optimizer on the STM6-40/36 module cell and SDM. The experiments' outcomes reveal that the I_SCHO algorithm exhibits superior performance based on its best RMSE 0.002506, worst RMSE 0.011506, and the very comparable SD value 0.72828. The implemented algorithm performs noticeably better than the other competitive algorithms by obtaining the minimum Root Mean Square Error (RMSE) as the fitness function.

In our experimental analysis, we utilized convergence curves as shown in Fig. 16a. The I_SCHO algorithm demonstrated minimized the RMSE, although saturation accurs after 400 trials, which is still better that HGS, in term of RMSE and time complexity. On the other hand, Fig. 16b and d prove high consistency between the measured actual values and the estimated values. Figure 16c states the robustness of the I_SCHO algorithm by achieving the least RMSE during the different 30 trials without any variations and oscillations as observed with other algorithms.

Experiments on double-diode model (DDM)-based USTM6-40/36 cell

This section shows the results of thirty trials on the DDM-based USTM6-40/36 utilising our suggested modified technique I_SCHO. The ideal parameters are shown in Table 16. The Table shows that the I_SCHO algorithm performs significantly better than all other approaches, achieving the lowest best and worst RMSE values and the lowest standard deviation (SD), which are 0.0016782 ,0.0030151, and 0.0002595, respectively.

Figure 17a demonstrates that the DDM-based trials saturated after number of trials same to SDM-based experiments, which approaches the original SCHO algorithm and ALO algorithm. Figure 17b and d show that the estimated and measured P-V and I-V characteristics are highly aligned. Furthermore, the measured RMSE values, shown in Fig. 17c, continuously approached the minimum, demonstrating the maintainabilty of the enhanced algorithm.

Experiments on triple-diode model (TDM)-based USTM6-40/36 cell

Finally, experiments were carried out to identify the ideal measured parameters for the TDM and USTM6-40/36 cell. Table 17 presents the results of the different algorithms and shows that, according to RMSE measurements, I_SCHO is the best-performing approach, which achieves 0.0017386, 0.0033737, and 0.00048366 for the best RMSE, worst RMSE, and SD, respectively. The table illustrates the improved performance of I_SCHO over the other algorithms by comparing the RMSE values, which were outperforming in terms of worst RMSE and standard deviation (SD) and highly near to those of the GWO algorithm in terms of best RMSE.

The convergence curves for each method are shown in Fig. 18a, which emphasizes the efficiency and outperformance of I_SCHO. This figure's analysis indicates that I_SCHO attains the lowest RMSE after about 250 iterations, which is faster than GWO. Although I_SCHO and GWO achieve almost the same best RMSE values,

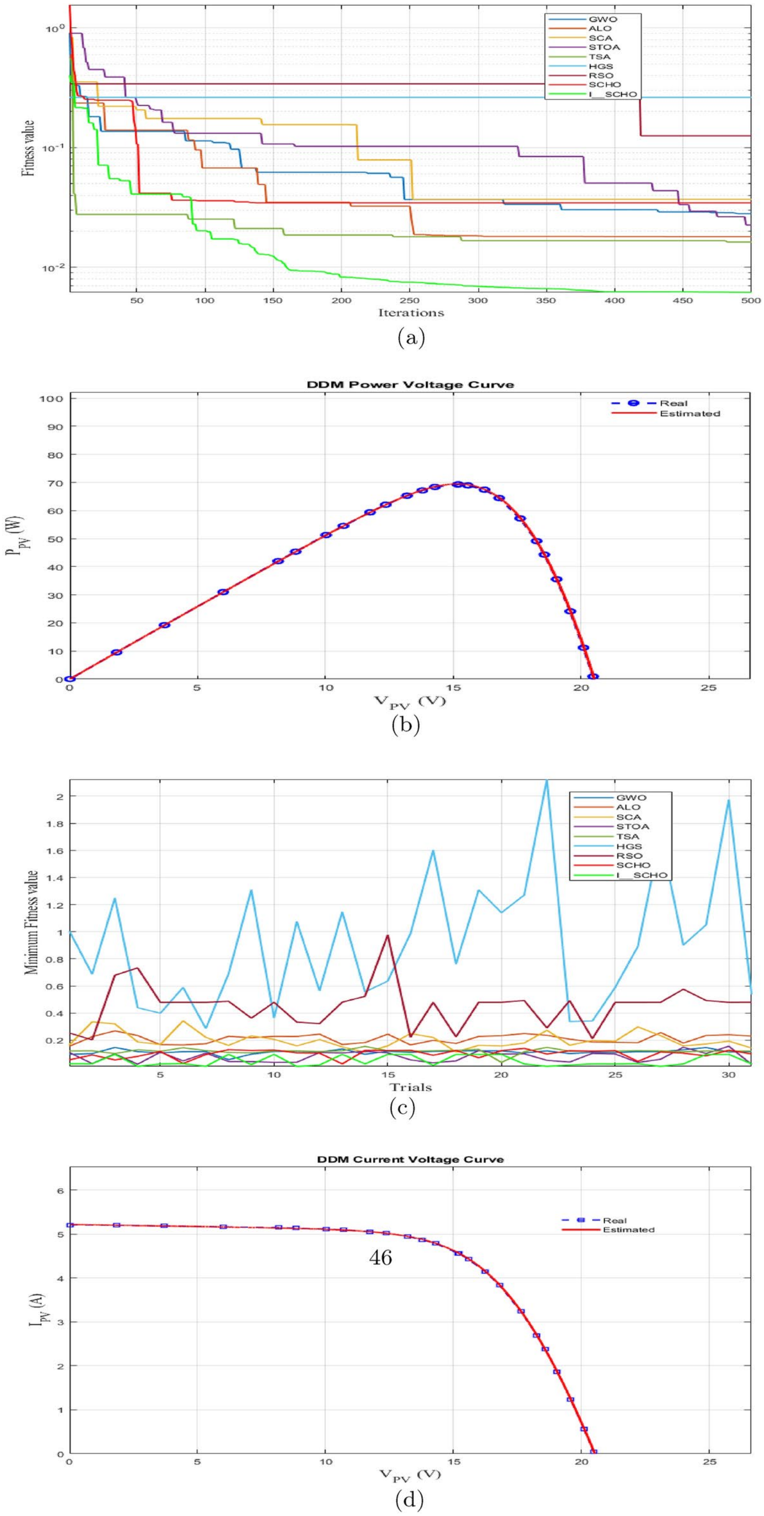

Fig. 14. Comparison between algorithms based on DDM and ultra 85-P W cell.

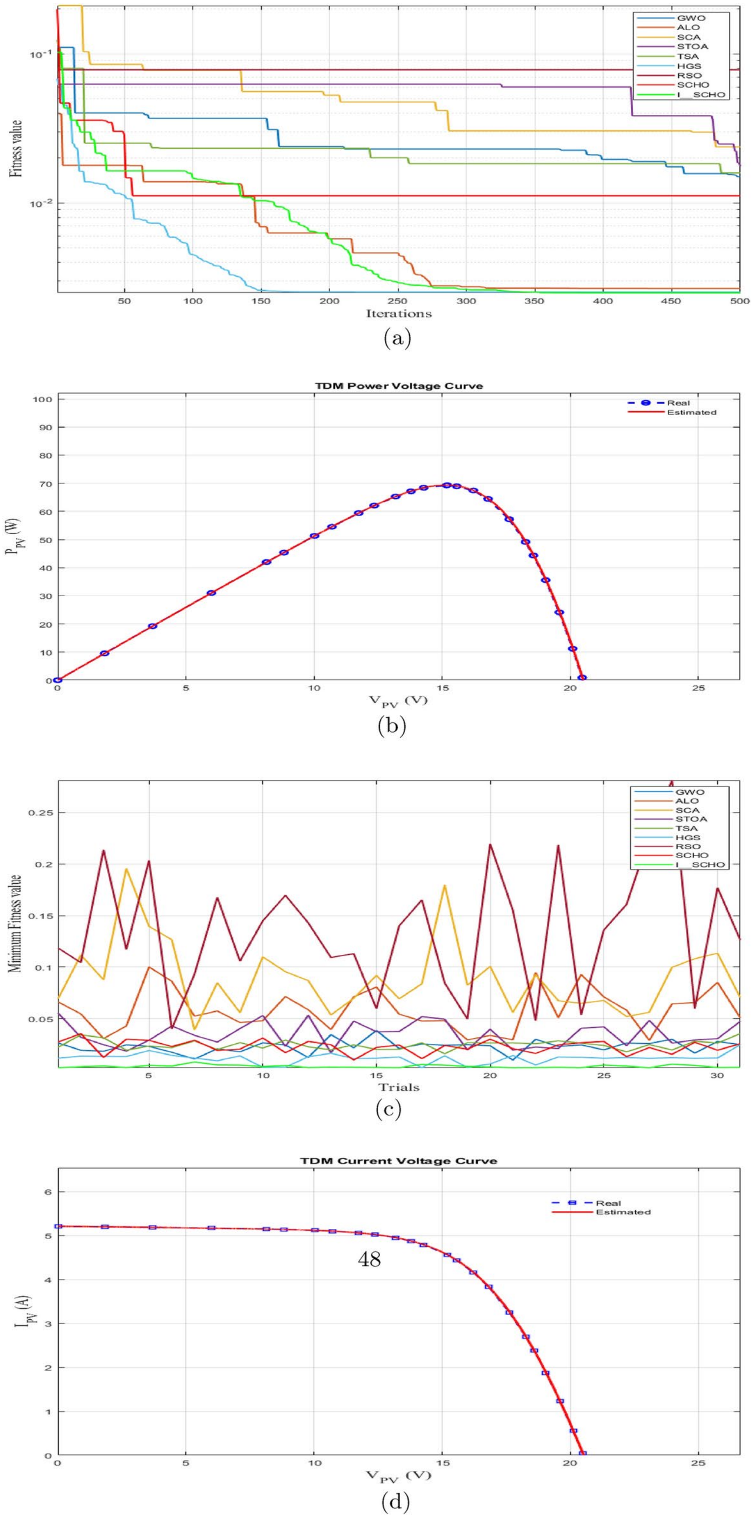

Fig. 15. Comparison between algorithms based on TDM and ultra 85-P W cell.

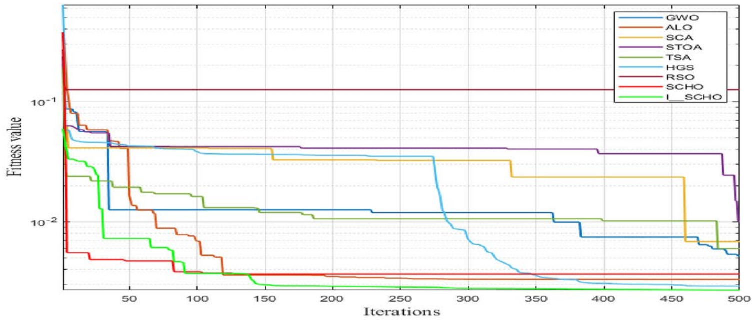

(a)

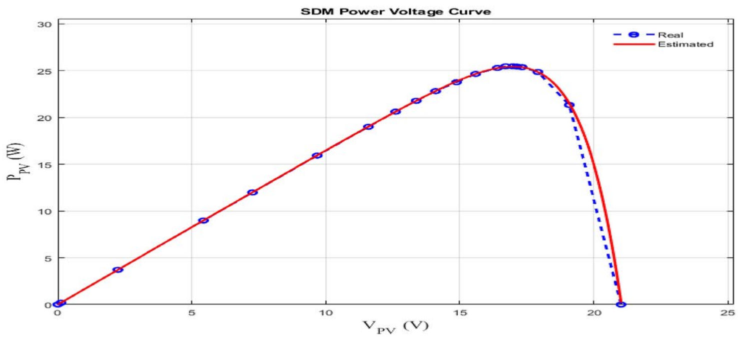

(b)

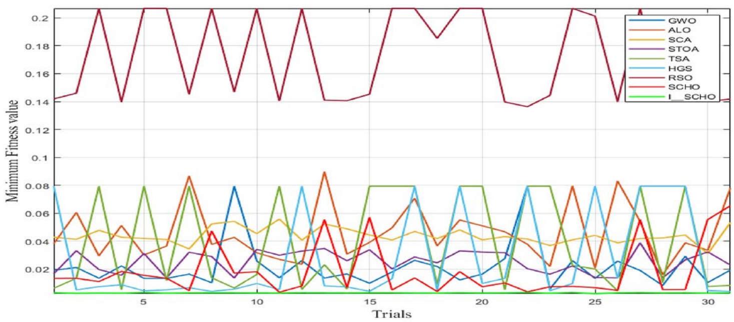

(c)

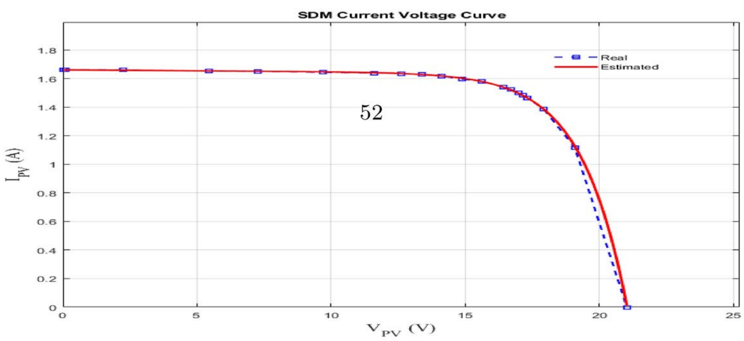

(d)

Fig. 16. Comparison between algorithms based on SDM and USTM6-40/36 cell.

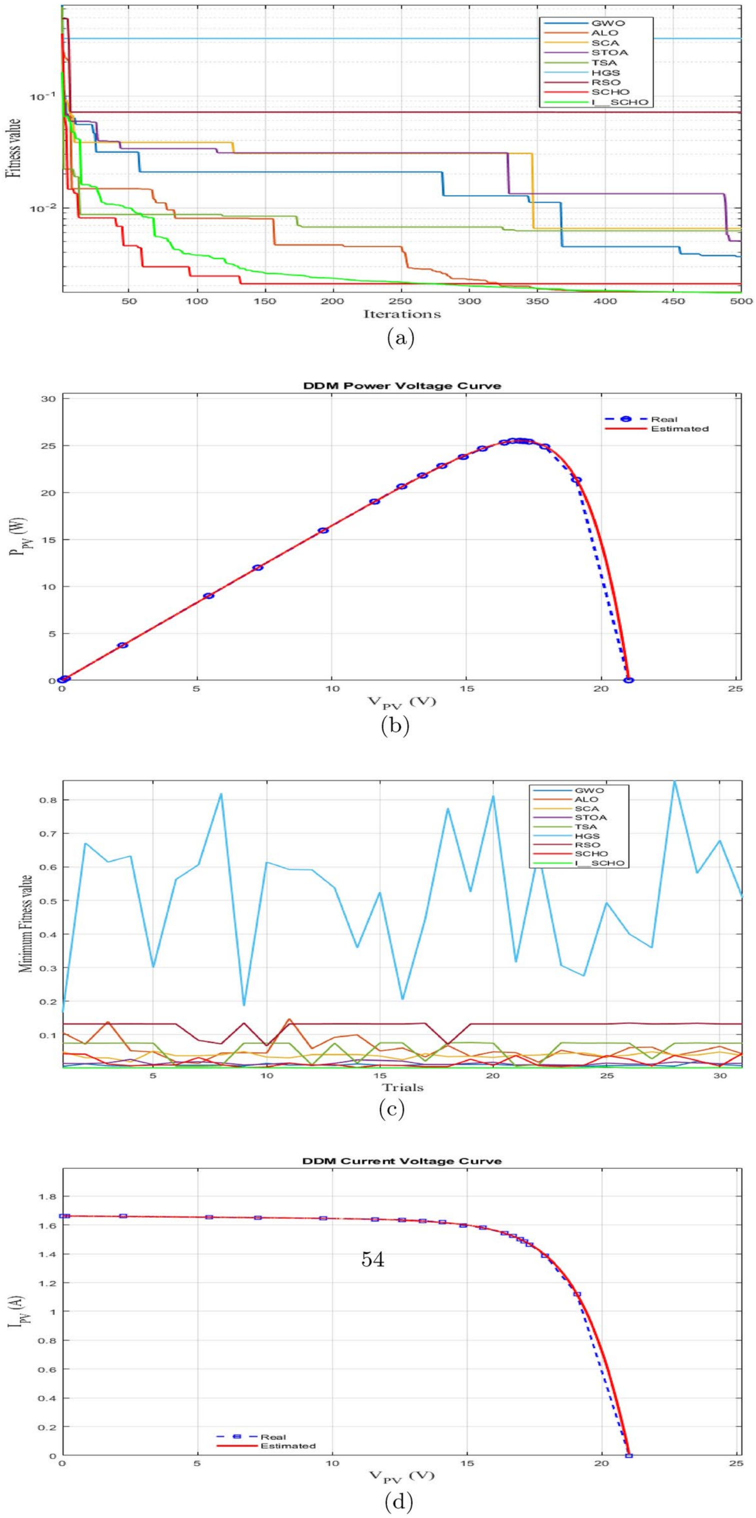

Fig. 17. Comparison between algorithms based on DDM and USTM6-40/36 cell.

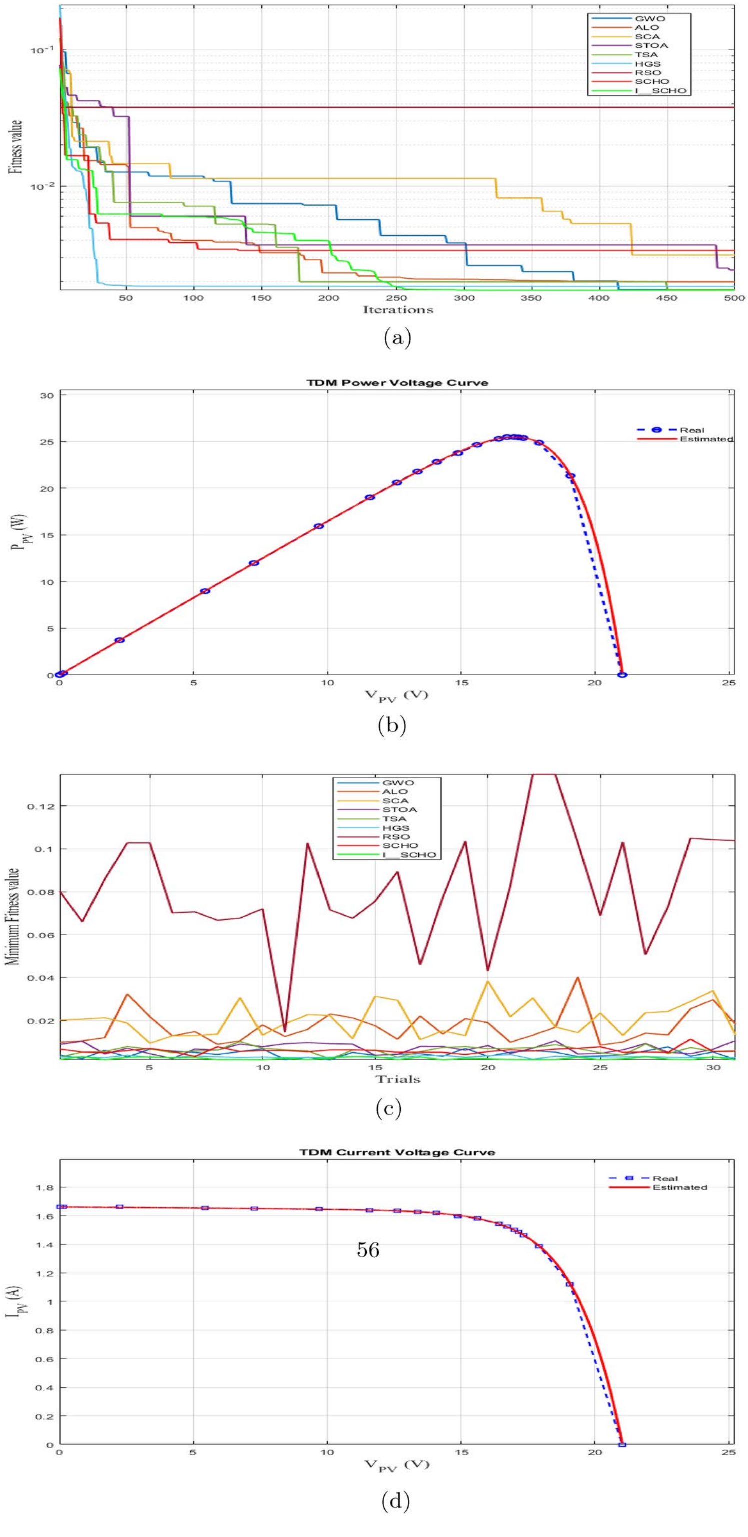

Fig. 18. Comparison between algorithms based on TDM and USTM6-40/36 cell.

I_SCHO reaches the optimum measurements faster, reducing the GWO saturation time. Again, high alignment is indicated in Fig. 18b and d between the measured and the estimated P-V and I-V characteristics, while Fig. 18c shows stability and robustness in continuously achieving the minimum RMSE over the 30 different trials.

Figure 19 compares the run times of the different algorithms participating in this comparative study. The graph is recorded on the RTC France cell using the SDM, DDM, and TDM models.

The average computational cost of I_SCHO using the SDM model is reported in Fig. 19a to be around 3 s. The Figure indicates that the average computation cost is comparable between I_SCHO, RSO, STOA, SCA, and GWO, but I_SCHO is the best. In "Experiments on single-diode mode based RTC France cell" section, it is noticed that I_SCHO achieved the best RMSE when compared to these competitive algorithms.

The computational time for the DDM model and RTC France cell is reported in Fig. 19b and is shown to be around 7 s, higher than the time recorded in the SDM and the TDM models. Concerning the DDM model, the time performance of I_SCHO is very comparable to SCHO, STOA, and SCA. In "RTC France cell" section, the I_SCHO achieved the best RMSE compared to these competitive algorithms.

Finally, Fig. 19c shows the average computational cost on the TDM around 3 s. The performance of the TDM model is very close to RSO, TSA, STOA, and SCA algorithms. On the other side, when referring to "RTC France cell" section, it is indicated that the RMSE values of RSO were the worst. While the RMSE values of the other algorithms were comparable to I_SCHO but not better, and the saturation of their curves was achieved later than the suggested algorithm I_SCHO.

Comparative analysis of robustness performance and statistical evaluation

The experiments were conducted on five different solar cells. These are the RTC France cell, Photowatt-PWP201 cell, Kyocera KC200GT - 204.6 W cell, Ultra 85-P cell, and STM6-40/36 module cell. On each cell, experiments were performed in three different modes. These modes are Single-Diode mode, Double-Diode mode, and Triple-Diode mode. Each experiment was applied to identify the optimal parameters of each cell. The optimization process is evaluated by measuring the best RMSE, worst RMSE, and the standard deviation. The performance of each optimizer is measured over 30 trials to measure each algorithm's stability and robustness. The differences between the estimated and calculated values were visualized in P-V and I-V graphs.

The I_SCHO algorithm, identified as the optimum algorithm, consistently outperformed or surpassed other algorithms across all performance metrics. During the 30 trials, the computed minimized Root Mean Square Error (RMSE) demonstrated its stability, sustainability, and potential to enhance the original SCHO algorithm significantly, demonstrating superior performance by achieving lower RMSE values. However, these improved results were attained after applying more trials, but on the other side, the runtime of I_SCHO was less than the runtime of SCHO. The figures representing the RMSE over the 30 trials indicate that the I_SCHO method achieved the lowest RMSE among the thirty trials. This demonstrates sustainability due to the lack of oscillations in the recorded RMSE values.

When experiments were conducted on the RTC France Cell, the achieved RMSE values of I_SCHO were comparable to those of the GWO and STOA algorithms when using the SDM and the TDM model. However, the best RMSE achieved was 0.0012518, the minimum achieved RMSE for all the algorithms. The worst RMSE recorded in the 30 trials of I_SCHO was 0.019984, which was also the most optimum relative to the other algorithms. While using the TDM model, results were comparable with algorithms that attained similar RMSE values, like SCA, HGS, and TSA. However, I_SCHO was faster in saturating to the best optimum RMSE among these considered algorithms. The I_SCHO outcomes are superior in terms of accuracy and reliability. According to our analysis of the results, the I_SCHO has the highest accuracy for the SDM, followed by the SCHO, TSA, GWO, HGS, ALO, SCA, RSO, and STOA in that order.

Experiments conducted on Photowatt-PWP201 cells showed that after 30 iterations, the I_SCHO algorithm achieved the best and worst RMSE and standard deviation (SD) values. The algorithm achieved the lowest RMSE and standard deviation (SD) while maintaining Fill Factor and Iphoto values, outperforming other state-of-the-art algorithms. The I_SCHO algorithm consistently achieved the lowest Root Mean Square Error (RMSE) within a satisfactory time frame, closely approximating the performance of the SCHO algorithm. The readings between the measured and estimated values for the P-V and I-V characteristics were identical. The I_SCHO algorithm's performance was on par with the TSA in terms of the number of trials required to reach saturation. In terms of the achieved RMSE values, the I_SCHO algorithm's performance was comparable to the GWO algorithm, demonstrating its effectiveness.

The saturation of the convergence curve during the DDM-based Kyocera KC200GT-204.6 W experiments was much faster than that of the SDM. The I_SCHO algorithm was the best-performing method among all tested, achieving the lowest RMSE after 370 iterations. Using the TDM model, the I_SCHO algorithm exhibits higher temporal complexity than HGS but demonstrates stability and achieves comparable RMSE values, outperforming all other algorithms. Experiments on the Ultra 85-P cell show that the I_SCHO algorithm exhibits saturates after more trials than HGS but demonstrates stability and achieves comparable RMSE values, outperforming all other algorithms. The strong convergence between the estimated and measured P-V and I-V characteristics emphasizes the algorithm's reliability. When optimizing the STM6-40/36 module cell with the I_SCHO algorithm, the convergence curves for each method highlight the efficiency and outperformance of I_SCHO. It achieves the lowest RMSE after 250 iterations, faster than GWO. The algorithm shows high alignment between measured and estimated P-V and I-V characteristics and its stability and robustness in achieving the minimum RMSE over 30 trials, providing reliable performance.

The experiments always show high alignment between the estimated P-V and the I-V characteristics and consistent RMSE, indicating stable and reliable performance. The convergence curve shows satisfactory iterations to reach the least RMSE. Convergence time is very comparable relative to the fastest algorithms. On the other hand, the best accuracy is achieved. Figure 19 states that the suggested algorithm, I_SCHO, reaches the

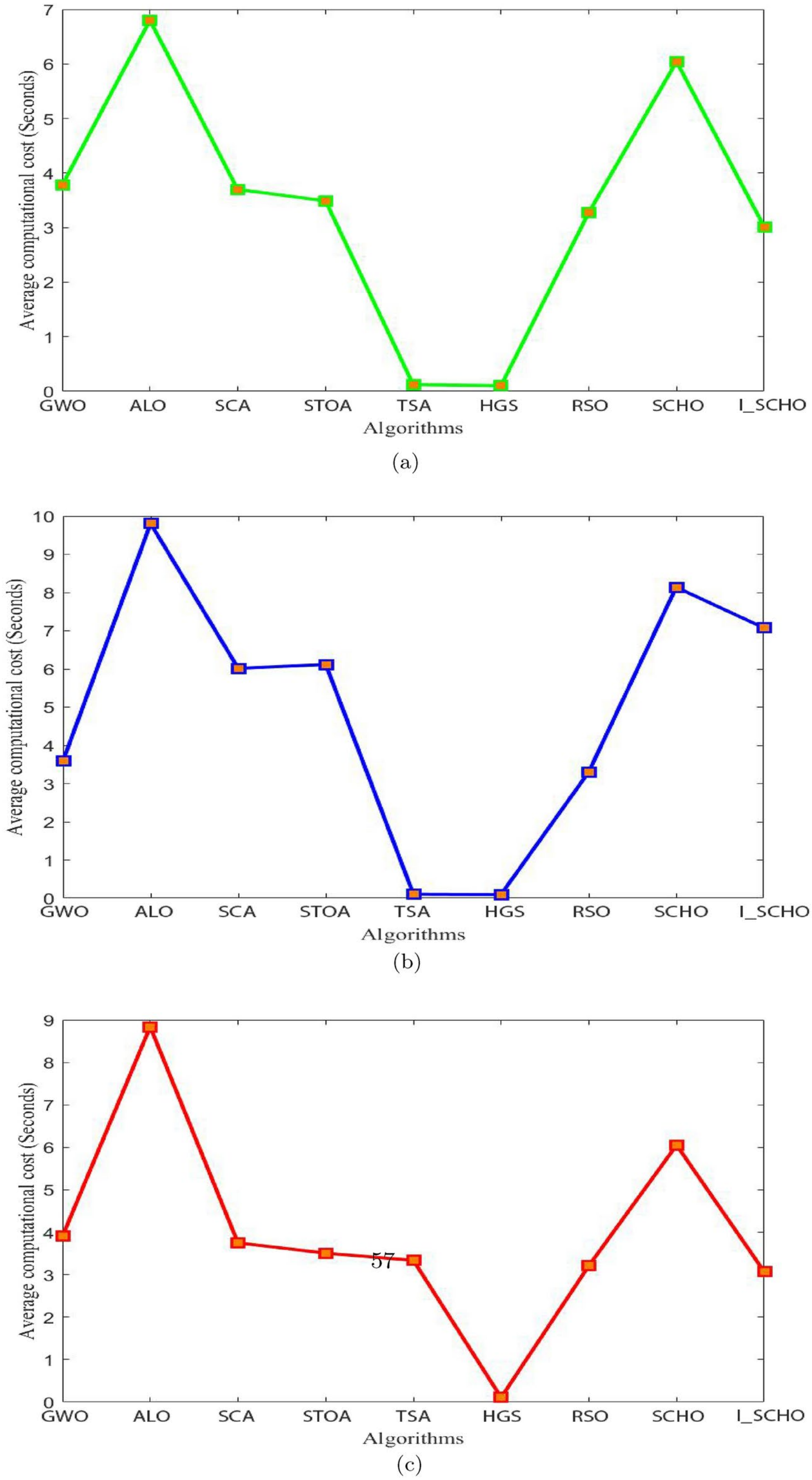

Fig. 19. Run time comparison between algorithms.

best-saturated RMSE in average computational time cost in seconds. The average computational time cost of the algorithm on SDM is reported in Fig. 19a to be around 3 s, while the DDM is reported in Fig. 19b to be around 7 s. Finally, Fig. 19c shows the average computational time cost on the TDM around 3 s.

Conclusion

The paper introduces an enhanced optimization algorithm, the Improved Sinh Cosh Optimizer (I_SCHO), for accurately modelling three solar PV model parameters. By integrating trigonometric operators from the Sine Cosine Algorithm into the exploitation phase of SCHO, the I_SCHO aims to avoid local optima and accelerate convergence towards the global optimum. This study demonstrates the algorithm's superior performance in parameter estimation, achieving the lowest root mean square error (RMSE) and standard deviation compared to established methods.

The I_SCHO was applied to three PV models (Single-Diode, Double-Diode, and Triple-Diode) across five solar cells, including RTC France, Photowatt-PWP201, Ultra 85-P, Kyocera KC200GT-204.6 W, and STM6-40/36. Results were compared with several algorithms. High alignment between estimated and actual P-V and I-V characteristics, along with consistent best RMSE values, demonstrates the robustness and reliability of the I_SCHO. While the convergence time is comparable to the fastest algorithms, the I_SCHO consistently achieves superior accuracy. The findings suggest that I_SCHO has significant potential to address optimization challenges in solar cell systems, offering a promising solution. Future research could explore its application in diverse domains, further enhancing its potential impact.

While this study demonstrates the effectiveness of the enhanced Sinh Cosh Optimizer (I_SCHO) in estimating parameters for single, double, and triple-diode photovoltaic (PV) models, several areas warrant further exploration. Future research could focus on extending the application of the I_SCHO algorithm to other PV models and technologies, such as thin-film and multi-junction cells, to assess its versatility and adaptability. Another interesting avenue would be to optimize the algorithm's parameters under varying environmental conditions, such as temperature fluctuations and partial shading, to enhance its real-world applicability.

Moreover, the integration of the I_SCHO algorithm with hardware-in-the-loop (HIL) simulations could provide more insights into its performance in real-time scenarios. Finally, conducting comprehensive experimental validations across a broader range of solar cells and PV modules would solidify the algorithm's robustness and ensure that it meets the practical demands of diverse PV systems. These future studies would not only refine the current algorithm but also contribute significantly to the field of PV parameter estimation and optimization.

The practical implementation of the enhanced Sinh Cosh Optimizer (I_SCHO) faces several limitations. The algorithm, while effective in improving accuracy and avoiding local optima, introduces added complexity that may increase computational costs, making it less suitable for real-time applications with limited resources. Further research and broader experimental testing are necessary to fully validate the algorithm's practicality and robustness in diverse scenarios.

Data availability

All data are available upon reasonable request from the corresponding author, Diaa Salama AbdElminaam.

Received: 18 April 2024; Accepted: 6 January 2025
Published online: 06 February 2025

References

1. Sachs, J. D. Achieving the sustainable development goals. *J. Int. Bus. Ethics* **8**(2), 53–62 (2015).
2. Premkumar, M. & Karthick, K. A review on solar PV based grid connected microinverter control schemes and topologies. *Int. J. Renew. Energy Dev.* **7**, 171. https://doi.org/10.14710/ijred.7.2.171-182 (2018).
3. Premkumar, M., Kumar, C. & Sowmya, R. Mathematical modelling of solar photovoltaic cell/panel/array based on the physical parameters from the manufacturers datasheet. *Int. J. Renew. Energy Dev.* **9**, 7–22 (2020).
4. Manoharan, P. et al. Improved perturb & observation maximum power point tracking technique for solar photovoltaic power generation systems (2020)
5. Calasan, M., Jovanovič̈, D., Rubež̈ïč̈, V., Mujovič̈, S. & Dukanovič̈, S. Estimation of single-diode and two-diode solar cell parameters by using a chaotic optimization approach. *Energies*. **12** (2019) https://doi.org/10.3390/en12214209
6. Moshksar, E. & Ghanbari, T. Adaptive estimation approach for parameter identification of photovoltaic modules. *IEEE J. Photovolt.* **7**, 614–623. https://doi.org/10.1109/JPHOTOV.2016.2633815 (2017).
7. Long, W., Cai, S., Jiao, J., Xu, M. & Wu, T. A new hybrid algorithm based on grey wolf optimizer and cuckoo search for parameter extraction of solar photovoltaic models. *Energy Convers.* (2020)
8. Premkumar, M., Sowmya, R., Umashankar, S. & Jangir, P. Extraction of uncertain parameters of single-diode photovoltaic module using hybrid particle swarm optimization and grey wolf optimization algorithm (2020).
9. Navabi, R., Abedi, S., Hosseinian, S. & Pal, R. On the fast convergence modeling and accurate calculation of pv output energy for operation and planning studies. *Energy Convers. Manag.* **89**, 497–506 (2015).
10. Li, S., Gong, W. & Gu, Q. A comprehensive survey on meta-heuristic algorithms for parameter extraction of photovoltaic models. *Renew. Sustain. Energy Rev.* **141**, 110828 (2021).
11. Jordehi, A. Parameter estimation of solar photovoltaic (pv) cells: a review. *Renew. Sustain. Energy Rev.* **61**, 354–371 (2016).
12. Yu, K., Liang, J., Qu, B., Cheng, Z. & Wang, H. Multiple learning backtracking search algorithm for estimating parameters of photovoltaic models. *Appl. Energy* **226**, 408–422 (2018).
13. Long, W., Wu, T., Xu, M., Tang, M. & Cai, S. Parameters identification of photovoltaic models by using an enhanced adaptive butterfly optimization algorithm. *Energy* **229**, 120750 (2021).
14. Calasan, M., Aleem, S. & Zobaa, A. On the root mean square error (rmse) calculation for parameter estimation of photovoltaic models: a novel exact analytical solution based on lambert w function. *Energy Convers. Manag.* **210**, 112716 (2020).
15. El-Fergany, A. Parameters identification of pv model using improved slime mould optimizer and lambert w-function. *Energy Rep.* **7**, 875–887 (2021).

16. Ridha, H. Parameters extraction of single and double diodes photovoltaic models using marine predators algorithm and lambert m function. *Sol. Energy* **209**, 674–693 (2020).
17. Gao, X., Cui, Y., Hu, J., Xu, G. & Yu, Y. Lambert w-function based exact representation for double diode model of solar cells: comparison on fitness and parameter extraction. *Energy Convers. Manag.* **127**, 443–460 (2016).
18. Easwarakhanthan, T., Bottin, J., Bouhouch, I. & Boutrit, C. Nonlinear minimization algorithm for determining the solar cell parameters with microcomputers. *Int. J. Solar Energy* **4**, 1–12 (1986).
19. Calasan, M., Aleem, S. & Zobaa, A. A new approach for parameters estimation of double and triple diode models of photovoltaic cells based on iterative lambert w function. *Sol. Energy* **218**, 392–412 (2021).
20. Ridha, H. et al. Parameters extraction of three diode photovoltaic models using boosted lshade algorithm and newton raphson method. *Energy* **224**, 120136 (2021).
21. Orioli, A. & Di Gangi, A. A procedure to calculate the five-parameter model of crystalline silicon photovoltaic modules on the basis of the tabular performance data. *Appl. Energy* **102**, 1160–1177 (2013).
22. Chan, D., Phillips, J. & Phang, J. A comparative study of extraction methods for solar cell model parameters. *Solid State Electron.* **29**, 329–337 (1986).
23. Zhang, Y., Ma, M. & Jin, Z. Backtracking search algorithm with competitive learning for identification of unknown parameters of photovoltaic systems. *Expert Syst. Appl.* **160**, 113750 (2020).
24. Kumar, C., Raj, T., Premkumar, M. & Raj, T. A new stochastic slime mould optimization algorithm for the estimation of solar photovoltaic cell parameters. *Optik* **223**, 165277 (2020).
25. Abdel-Basset, M., El-Shahat, D., Chakrabortty, R. & Ryan, M. Parameter estimation of photovoltaic models using an improved marine predators algorithm. *Energy Convers. Manag.* **227**, 113491 (2021).
26. Soliman, M., Hasanien, H. & Alkuhayli, A. Marine predators algorithm for parameters identification of triple-diode photovoltaic models. *IEEE Access* **8**, 155832–842 (2020).
27. Yang, X. & Gong, W. Opposition-based jaya with population reduction for parameter estimation of photovoltaic solar cells and modules. *Appl. Soft Comput.* **104**, 107218 (2021).
28. Yu, K. et al. A performance-guided jaya algorithm for parameters identification of photovoltaic cell and module. *Appl. Energy* **237**, 241–257 (2019).
29. Zhang, Y., Ma, M. & Jin, Z. Comprehensive learning jaya algorithm for parameter extraction of photovoltaic models. *Energy* **211**, 118644 (2020).
30. Abdel-Basset, M., Mohamed, R., Chakrabortty, R., Ryan, M. & El-Fergany, A. An improved artificial jellyfish search optimizer for parameter identification of photovoltaic models. *Energies* **14**, 1867 (2021).
31. Liang, J. et al. Parameters estimation of solar photovoltaic models via a self-adaptive ensemble-based differential evolution. *Sol. Energy* **207**, 336–346 (2020).
32. Li, S., Gu, Q., Gong, W. & Ning, B. An enhanced adaptive differential evolution algorithm for parameter extraction of photovoltaic models. *Energy Convers. Manag.* **205**, 112443 (2020).
33. Qais, M., Hasanien, H., Alghuwainem, S. & Nouh, A. Coyote optimization algorithm for parameters extraction of three-diode photovoltaic models of photovoltaic modules. *Energy* **187**, 116001 (2019).
34. Ibrahim, I., Hossain, M., Duck, B. & Nadarajah, M. An improved wind-driven optimization algorithm for parameters identification of a triple-diode photovoltaic cell model. *Energy Convers. Manag.* **213**, 112872 (2020).
35. Pardhu, B. & Kota, V. Radial movement optimization based parameter extraction of double diode model of solar photovoltaic cell. *Sol. Energy* **213**, 312–327 (2021).
36. Abdel-Basset, M., Mohamed, R., Chakrabortty, R., Sallam, K. & Ryan, M. An efficient teaching-learning-based optimization algorithm for parameters identification of photovoltaic models: analysis and validations. *Energy Convers. Manag.* **227**, 113614 (2021).
37. Mokeddem, D. Parameter extraction of solar photovoltaic models using enhanced levy flight based grasshopper optimization algorithm. *J. Electr. Eng. Technol.* **16**, 171–179 (2021).
38. Qais, M., Hasanien, H. & Alghuwainem, S. Parameters extraction of three-diode photovoltaic model using computation and harris hawks optimization. *Energy* **195**, 117040 (2020).
39. Chen, H., Jiao, S., Wang, M., Heidari, A. & Zhao, X. Parameters identification of photovoltaic cells and modules using diversification-enriched harris hawks optimization with chaotic drifts. *J. Clean. Prod.* **244**, 118778 (2020).
40. Abdel-Basset, M., Mohamed, R., Mirjalili, S., Chakrabortty, R. & Ryan, M. Solar photovoltaic parameter estimation using an improved equilibrium optimizer. *Sol. Energy* **209**, 694–708 (2020).
41. Pires Deotti, L., Rezende Pereira, J. & Silva Junior, I. Parameter extraction of photovoltaic models using an enhanced levy flight bat algorithm. *Energy Convers. Manag.* **221**, 113114 (2020).
42. Gude, S. & Jana, K. Parameter extraction of photovoltaic cell using an improved cuckoo search optimization. *Sol. Energy* **204**, 280–293 (2020).
43. Qais, M. H., Hasanien, H. M. & Alghuwainem, S. Transient search optimization for electrical parameters estimation of photovoltaic module based on datasheet values. *Energy Convers. Manag.* **214**, 112904 (2020).
44. Zhang, H. et al. Orthogonal nelder-mead moth flame method for parameter identification of photovoltaic modules. *Energy Convers. Manag.* **211**, 112764 (2020).
45. Yousri, D., Thanikanti, S., Allam, D., Ramachandaramurthy, V. & Etiba, M. Fractional chaotic ensemble particle swarm optimizer for identifying the single, double, and three diode photovoltaic models' parameters. *Energy* **195**, 116979 (2020).
46. Lin, X. & Wu, Y. Parameters identification of photovoltaic models using niche-based particle swarm optimization in parallel computing architecture. *Energy* **196**, 117054 (2020).
47. Ridha, H., Gomes, C. & Hizam, H. Estimation of photovoltaic module model's parameters using an improved electromagnetic-like algorithm. *Neural Comput. Appl.* **32**, 12627–12642 (2020).
48. Diab, A. et al. Tree growth based optimization algorithm for parameter extraction of different models of photovoltaic cells and modules. *IEEE Access* **8**, 119668–119687 (2020).
49. Qais, M., Hasanien, H. & Alghuwainem, S. Identification of electrical parameters for three-diode photovoltaic model using analytical and sunflower optimization algorithm. *Appl. Energy* **250**, 109–117 (2019).
50. Long, W., Wu, T., Jiao, J., Tang, M. & Xu, M. Refraction-learning-based whale optimization algorithm for high-dimensional problems and parameter estimation of pv model. *Eng. Appl. Artif. Intell.* **89**, 103457 (2020).
51. Xiong, G., Zhang, J., Shi, D. & He, Y. Parameter extraction of solar photovoltaic models using an improved whale optimization algorithm. *Energy Convers. Manag.* **174**, 388–405 (2018).
52. Oliva, D., Abd El Aziz, M. & Hassanien, A. Parameter estimation of photovoltaic cells using an improved chaotic whale optimization algorithm. *Appl. Energy* **200**, 141–154 (2017).
53. Subudhi, B. & Pradhan, R. Bacterial foraging optimization approach to parameter extraction of a photovoltaic module. *IEEE Trans. Sustain. Energy* **9**, 381–389 (2018).
54. Wu, Z., Yu, D. & Kang, X. Parameter identification of photovoltaic cell model based on improved ant lion optimizer. *Energy Convers. Manag.* **151**, 107–115 (2017).
55. Lin, P., Cheng, S., Yeh, W., Chen, Z. & Wu, L. Parameters extraction of solar cell models using a modified simplified swarm optimization algorithm. *Sol. Energy* **144**, 594–603 (2017).

56. Jamadi, M., Merrikh-Bayat, F. & Bigdeli, M. Very accurate parameter estimation of single-and double-diode solar cell models using a modified artificial bee colony algorithm. *Int. J. Energy Environ. Eng.* **7**, 13–25 (2016).
57. Bastidas-Rodriguez, J., Petrone, G., Ramos-Paja, C. & Spagnuolo, G. A genetic algorithm for identifying the single diode model parameters of a photovoltaic panel. *Math. Comput. Simul.* **131**, 38–54 (2017).
58. Niu, Q., Zhang, L. & Li, K. A biogeography-based optimization algorithm with mutation strategies for model parameter estimation of solar and fuel cells. *Energy Convers. Manag.* **86**, 1173–1185 (2014).
59. Chen, H. et al. An opposition-based sine cosine approach with local search for parameter estimation of photovoltaic models. *Energy Convers. Manag.* **195**, 927–942 (2019).
60. Abbassi, A. et al. Parameters identification of photovoltaic cell models using enhanced exploratory salp chains-based approach. *Energy* **198**, 117333 (2020).
61. Kler, D., Sharma, P., Banerjee, A., Rana, K. & Kumar, V. Pv cell and module efficient parameters estimation using evaporation rate based water cycle algorithm. *Swarm Evol. Comput.* **35**, 93–110 (2017).
62. Askarzadeh, A. & Coelho, L. Determination of photovoltaic modules parameters at different operating conditions using a novel bird mating optimizer approach. *Energy Convers. Manag.* **89**, 608–614 (2015).
63. Fathy, A. & Rezk, H. Parameter estimation of photovoltaic system using imperialist competitive algorithm. *Renew. Energy* **111**, 307–320 (2017).
64. Ali, E., El-Hameed, M., El-Fergany, A. & El-Arini, M. Parameter extraction of photovoltaic generating units using multi-verse optimizer. *Sustain. Energy Technol. Assess.* **17**, 68–76 (2016).
65. Mirjalili, S., Mirjalili, S. M. & Lewis, A. Grey wolf optimizer. *Adv. Eng. Softw.* **69**, 46–61 (2014).
66. Mirjalili, S. Sca: a sine cosine algorithm for solving optimization problems. *Knowl.-Based Syst.* **96**, 120–133 (2016).
67. Dhiman, G. & Kaur, A. Stoa: a bio-inspired based optimization algorithm for industrial engineering problems. *Eng. Appl. Artif. Intell.* **82**, 148–174 (2019).
68. Kaur, S., Awasthi, L. K., Sangal, A. & Dhiman, G. Tunicate swarm algorithm: A new bio-inspired based metaheuristic paradigm for global optimization. *Eng. Appl. Artif. Intell.* **90**, 103541 (2020).
69. Mehta, P., Yildiz, B. S., Sait, S. M. & Yildiz, A. R. Hunger games search algorithm for global optimization of engineering design problems. *Mater. Test.* **64**(4), 524–532 (2022).
70. Houssein, E. H., Hosney, M. E., Oliva, D., Younis, E. M., Ali, A. A., & Mohamed, W. M. An efficient discrete rat swarm optimizer for global optimization and feature selection in chemoinformatics. *Knowl.-Based Syst.* 110697 (2023)
71. Dehghani, M. & Trojovskỳ, P. Osprey optimization algorithm: A new bio-inspired metaheuristic algorithm for solving engineering optimization problems. *Front. Mech. Eng.* **8**, 1126450 (2023).
72. A sinh cosh optimizer. *Knowl.-Based Syst.* **282**, 111081 https://doi.org/10.1016/j.knosys.2023.111081 (2023).

Acknowledgements
The authors would like to acknowledge the support of Princess Nourah bint Abdulrahman University Researchers Supporting Project number (PNURSP2025R435), Princess Nourah bint Abdulrahman University, Riyadh, Saudi Arabia.

Author contributions
All authors contributed equally to this paper. All authors read and approved the final paper.

Funding
The authors would like to acknowledge the support of Princess Nourah bint Abdulrahman University Researchers Supporting Project number (PNURSP2025R435), Princess Nourah bint Abdulrahman University, Riyadh, Saudi Arabia.

Declarations

Competing interests
The authors declare no competing interests.

Additional information
Correspondence and requests for materials should be addressed to D.S.A.